NUREG/IA-0234

International Agreement Report

Analysis of a Loss of Normal Feedwater Transient at the Ringhals-3 NPP Using RELAP5/Mod3.3

Prepared by:
J. Bánáti, C. Demaziére, and M. Stålek

Chalmers University of Technology
Department of Nuclear Engineering
S-41296 Gothenburg, SWEDEN

A. Calvo, NRC Project Manager

Office of Nuclear Regulatory Research
U.S. Nuclear Regulatory Commission
Washington, DC 20555-0001

July 2010

Prepared as part of
The Agreement on Research Participation and Technical Exchange
Under the Thermal-Hydraulic Code Applications and Maintenance Program (CAMP)

Published by
U.S. Nuclear Regulatory Commission

AVAILABILITY OF REFERENCE MATERIALS IN NRC PUBLICATIONS

NRC Reference Material

As of November 1999, you may electronically access NUREG-series publications and other NRC records at NRC's Public Electronic Reading Room at http://www.nrc.gov/reading-rm.html. Publicly released records include, to name a few, NUREG-series publications; *Federal Register* notices; applicant, licensee, and vendor documents and correspondence; NRC correspondence and internal memoranda; bulletins and information notices; inspection and investigative reports; licensee event reports; and Commission papers and their attachments.

NRC publications in the NUREG series, NRC regulations, and *Title 10, Energy*, in the Code of *Federal Regulations* may also be purchased from one of these two sources.

1. The Superintendent of Documents
   U.S. Government Printing Office
   Mail Stop SSOP
   Washington, DC 20402-0001
   Internet: bookstore.gpo.gov
   Telephone: 202-512-1800
   Fax: 202-512-2250
2. The National Technical Information Service
   Springfield, VA 22161-0002
   www.ntis.gov
   1-800-553-6847 or, locally, 703-605-6000

A single copy of each NRC draft report for comment is available free, to the extent of supply, upon written request as follows:

Address: Office of the Chief Information Officer,
Reproduction and Distribution
Services Section
U.S. Nuclear Regulatory Commission
Washington, DC 20555-0001
E-mail: DISTRIBUTION@nrc.gov
Facsimile: 301-415-2289

Some publications in the NUREG series that are posted at NRC's Web site address http://www.nrc.gov/reading-rm/doc-collections/nuregs are updated periodically and may differ from the last printed version. Although references to material found on a Web site bear the date the material was accessed, the material available on the date cited may subsequently be removed from the site.

Non-NRC Reference Material

Documents available from public and special technical libraries include all open literature items, such as books, journal articles, and transactions, *Federal Register* notices, Federal and State legislation, and congressional reports. Such documents as theses, dissertations, foreign reports and translations, and non-NRC conference proceedings may be purchased from their sponsoring organization.

Copies of industry codes and standards used in a substantive manner in the NRC regulatory process are maintained at—

The NRC Technical Library
Two White Flint North
11545 Rockville Pike
Rockville, MD 20852-2738

These standards are available in the library for reference use by the public. Codes and standards are usually copyrighted and may be purchased from the originating organization or, if they are American National Standards, from—

American National Standards Institute
11 West 42nd Street
New York, NY 10036-8002
www.ansi.org
212-642-4900

Legally binding regulatory requirements are stated only in laws; NRC regulations; licenses, including technical specifications; or orders, not in NUREG-series publications. The views expressed in contractor-prepared publications in this series are not necessarily those of the NRC.

The NUREG series comprises (1) technical and administrative reports and books prepared by the staff (NUREG–XXXX) or agency contractors (NUREG/CR–XXXX), (2) proceedings of conferences (NUREG/CP–XXXX), (3) reports resulting from international agreements (NUREG/IA–XXXX), (4) brochures (NUREG/BR–XXXX), and (5) compilations of legal decisions and orders of the Commission and Atomic and Safety Licensing Boards and of Directors' decisions under Section 2.206 of NRC's regulations (NUREG–0750).

DISCLAIMER: This report was prepared as an account of work sponsored by an agency of the U.S. Government. Neither the U.S. Government nor any agency thereof, nor any employee, makes any warranty, expressed or implied, or assumes any legal liability or responsibility for any third party=s use, or the results of such use, of any information, apparatus, product, or process disclosed in this publication, or represents that its use by such third party would not infringe privately owned rights.

NUREG/IA-0234

Analysis of a Loss of Normal Feedwater Transient at the Ringhals-3 NPP Using RELAP5/Mod3.3

Manuscript Completed: May 2010

Date Published: June 2010

Prepared by: József Bánáti, Christophe Demazière and Mathias Stålek

Chalmers University of Technology

Department of Nuclear Engineering

S-41296 Gothenburg, SWEDEN

U.S. Nuclear Regulatory Commission

Washington, DC 20555-0001

ABSTRACT

This report gives an account on the development and validation of the RELAP5/Mod3.3 model of the Ringhals-3 pressurized water reactor against a Loss of Normal Feedwater Transient, which occurred on August 16, 2005. The 3rd unit of Ringhals Nuclear Power Plant comprises a 3-loops Westinghouse design pressurized water reactor on the Swedish West Coast.

At first, the RELAP5 model is presented. All the 157 fuel assemblies are modeled individually in the code input. The model is furthermore able to handle possible asymmetrical conditions of the flow velocity and temperature fields between the loops.

The transient was initiated by a malfunction of the feedwater valve at the 2nd steam generator. Consequently, the turbines were tripped and, due to the low level in the SG-2 the reactor was scrammed. Activation of the auxiliary feedwater provided proper amount of cooling from the secondary side, resulting in safe shutdown conditions. Capabilities of the RELAP5 code were challenged in this transient. The calculated values of the parameters show good agreement with the measured data.

A parametric study was performed In order to evaluate the dependence of the steam generator level on the injected auxiliary feedwater flow. It indicated that the turbine driven auxiliary feedwater pump could possibly inject at a higher flowrate than its nominal value.

The work was performed by the Department of Nuclear Engineering, Chalmers University of Technology in the framework of the Ringhals-3 power uprate project, supported by the Swedish Radiation Safety Authority (SSM). The ultimate goal of this project is to perform independent safety analyses of some limiting transients associated to the power uprate. The work carried out so far was targeted towards the development of state-of-the-art modelling capabilities for the Ringhals-3 unit.

The present validational study is a Swedish contribution to the international Code Assessment and Maintenance Program (CAMP).

CONTENTS

Page

ABSTRACT III

CONTENTS V

FIGURES VII

TABLES VIII

FOREWORD IX

ACKNOWLEDGMENT X

ABBREVIATIONS XI

1. INTRODUCTION 1-1

2. DESCRIPTION OF THE TRANSIENT 2-1

3. FEATURES OF THE RELAP5 MODEL 3-1
   3.1 Status of the Model Development 3-1
   3.2 Description of the Nodalization 3-1
      3.2.1 The downcomer 3-4
      3.2.2 The lower plenum 3-4
      3.2.3 The core inlet 3-4
      3.2.4 The core 3-4
      3.2.5 The bypass channels 3-6
      3.2.6 The upper plenum 3-6
      3.2.7 The hot and cold legs 3-6
      3.2.8 The pressurizer 3-6
      3.2.9 The SG primary side 3-6
      3.2.10 The main circulation pumps 3-7
      3.2.11 The safety systems 3-7
      3.2.12 The feedwater system 3-7
      3.2.13 The Steam Generators 3-7
      3.2.14 The Steam Line 3-7
      3.2.15 Turbines and steam dump systems 3-9

4. RESULTS OF THE BASE CASE CALCULATIONS 4-1
   4.1 Reaching steady-state 4-1
   4.2 Transient results 4-7

5. PARAMETRIC STUDY ON THE AUXILIARY FEEDWATER FLOW 5-1

6. RUN STATISTICS 6-1
6.1 Remarks on the SNAP Graphical Tool 6-3

7. CONCLUSIONS 7-1

8. REFERENCES 8-1

Figures

Page

1. The Ringhals Nuclear Power Plant with 1 BWR and 3 PWR units....1-1
2. Nuclear facilities in Northern Europe....1-2
3. Narrow range levels in the upper part of SG 2....2-1
4. Nodalization of the reactor pressure vessel internals....3-2
5. Nodalization of the primary side....3-3
6. Numbering scheme of the fuel channels in radial sectors....3-4
7. Radial mesh points and material compositions in the fuel elements....3-5
8. Relative axial power distribution....3-5
9. Nodalization of the secondary side....3-8
10. Steady-state search of primary loop flowrate....4-2
11. Steady-state search of feedwater mass flowrate....4-2
12. Steady-state search of steam mass flowrate....4-3
13. Steady-state search of narrow range SG level....4-3
14. Steady-state search of pressures in the steam line....4-4
15. Steady-state PRZ pressure provided by a boundary volume....4-4
16. Steady-state search of coldleg temperatures....4-5
17. Steady-state search of hotleg temperatures....4-5
18. Feedwater mass flowrate to the malfunctioning SG-2....4-7
19. Narrow range level in the malfunctioning SG-2....4-8
20. Wide range level in the malfunctioning SG-2....4-8
21. The measured neutronic power and the relative heating power....4-9
22. Pressure in the intact SG-1....4-10
23. Pressure in the malfunctioning SG-2....4-10
24. Steam mass flowrate in steamline 1....4-11
25. Steam mass flowrate in steamline 2....4-12
26. Narrow range level in the intact SG-1....4-13
27. Narrow range level in the intact SG-3....4-13
28. Auxiliary feedwater flow to the intact SG-1 (given as BC)....4-14
29. Auxiliary feedwater flow to the intact SG-3 (nominal value is given as BC)....4-14
30. Coldleg temperature in the intact loop 1....4-16
31. Coldleg temperature in the malfunctioning loop 2....4-16
32. Hotleg temperature in the intact loop 1....4-17
33. Hotleg temperature in the malfunctioning loop 2....4-17
34. Level in the pressurizer....4-18
35. Pressure in the pressurizer....4-18
36. Arrangement of the normal and auxiliary feedwater system....5-1
37. AFW mass flowrate as varied parameter (boundary condition)....5-2
38. SG-3 level with various AFW injections....5-2
39. CPU time....6-2
40. Actual and Courant time steps....6-2
41. Mass error....6-3
42. Animation mask with fluid conditions and temperatures....6-4
43. Animation mask with void fractions....6-5

Tables

Page

1. Sequence of events during the transient 2-2
2. Comparison of calculated and measured steady-state parameters 4-6
3. Summary of the components in the model 6-1

FOREWORD

The present code assessment report was prepared with the intention to provide feedback to the developers and the user community of the NRC computer codes in order to demonstrate the capabilities of RELAP5/Mod3.3 Patch 3. The authors made intensive efforts to build an up-to-date model of the Ringhals-3 unit for analyses of transients using best estimate methods. As the results reveal in the current document, the code has successfully been validated against an operational transient that occurred in the relevant NPP.

I am convinced that the modeling strategies and main conclusions in this study will contribute to better understanding of a number of key thermal-hydraulic phenomena and will broaden the knowledge-base of safety authorities, as well as that of the code users worldwide.

Prof. Imre Pázsit
Department of Nuclear Engineering
Chalmers University of Technology
Gothenburg, Sweden

ACKNOWLEDGMENT

The following people are acknowledged for the help/feedback/comments they provided during the completion of the calculations in the relevant project: Magnus Holmgren and Kjell Ringdahl from Ringhals AB; Anders Sjöberg from Studsvik Nuclear, Oddbjörn Sandervåg and Ninos Garis at SSM.

ABBREVIATIONS

AFW	Auxiliary Feedwater
ANS	American Nuclear Society
BC	Boundary Condition
BWR	Boiling Water Reactor
CAMP	Code Assessment and Maintenance Program
CL	Cold Leg
DC	Downcomer
ECC	Emergency Core Cooling
FA	Fuel Assembly
FW	Feedwater
HL	Hot Leg
LONF	Loss of Normal Feedwater
MSIV	Main Steam Isolation Valve
NPP	Nuclear Power Plant
NR	Narrow Range
NSSS	Nuclear Steam Supply System
PLS	Precautions, Limitations and Setpoints
PWR	Pressurized Water Reactor
PRZ	Pressurizer
RELAP	Reactor Excursion and Leakage Analysis Program
RHR	Residual Heat Removal
RPV	Reactor Pressure Vessel
SG	Steam Generator
SKI	Swedish Nuclear Power Inspectorate
SL	Steam Line
SNAP	Symbolic Nuclear Analysis Package
SSM	Swedish Radiation Safety Authority (formerly known as SKI)
WR	Wide Range

1. INTRODUCTION

Many power utilities worldwide are applying for power uprates, i.e. for increasing the power output of their reactors. The Swedish Radiation Safety Authority (SSM, formerly known as the Swedish Nuclear Safety Inspectorate, SKI) received applications for new power uprates in Sweden, and among others, an application related to the Ringhals-3 Pressurized Water Reactor (Figure 1) in March 2004 [1]. This unit is a 3-loop Westinghouse type reactor, situated at the western coast of Sweden, approx. 60 km to the south of Gothenburg (Figure 2) [2].

Figure 1 The Ringhals Nuclear Power Plant with 1 BWR and 3 PWR units

Increase of the thermal power in Ringhals-3 was planned to be carried out in two steps. During the first step, the thermal power will be increased from 2783 MWth (e.g. the original NSSS power level, 100%) to 3000 MWth (108%). For the second step of the power uprate, the thermal power will be increased from 3000 MWth (108%) to 3160MWth (113.5%).

It is essential to identify the main consequences resulting from the increased power level of the reactor, and their impact on the safety of the plant. SSM has to decide whether such power uprates still fulfill the requirements for a safe operation of the Ringhals-3 PWR. Performing an independent safety analysis of the Ringhals-3 power uprate was thus given by SSM as a research project to the Department of Nuclear Engineering, Chalmers University of Technology.

Before stepping forward with the safety evaluation at an uprated power, a thermal-hydraulic model had to be created, updated and verified for the plant. With this objective in mind, a real operational transient, a Loss of Normal Feedwater case was chosen as a basis for validation of the model. By demonstration of the achievements and the shortcomings of the simulation, the authors intended to contribute to broadening of the knowledge base of the safety authority, as well as of the code user community.

Figure 2 Nuclear facilities in Northern Europe

2. DESCRIPTION OF THE TRANSIENT

The feedwater control valves of the Ringhals-3 Unit were retrofitted during the outage in 2005 and, among others they were equipped with new digital valve positioners. The feedwater valves were tested after the outage and everything worked properly. On August 16th 2005, however, an electrical filter in the position transducer malfunctioned and therefore, the control signal to the valve failed. In such a case the valve immediately closes since that is the safe position of the valve. As a result, the normal feedwater (FW) flow to the steam generator (SG) becomes blocked.

Initially, the lack of feedwater of SG-2 resulted in an increased amount of feedwater to the other two SGs before the safety and control systems were actuated. The steam production of the SG-2 was temporarily higher due to practically zero water inflow, while the heating power remained the same from the primary side. This change was represented by an increased primary system temperature and consequently, a higher pressurizer (PRZ) level and pressure.

The level in the malfunctioning SG started to drop rapidly. At 38 s after shutting off the FW valve it reached the setpoint of the reactor trip, which is 12.4 % of narrow range span (Figure 3). The SCRAM signal triggered the control rods mechanism and the reactor was shut down. The trip logic and the control system provided a standardized procedure for such a case, including the trip of the turbines, and a simultaneous actuation of the auxiliary feedwater system.

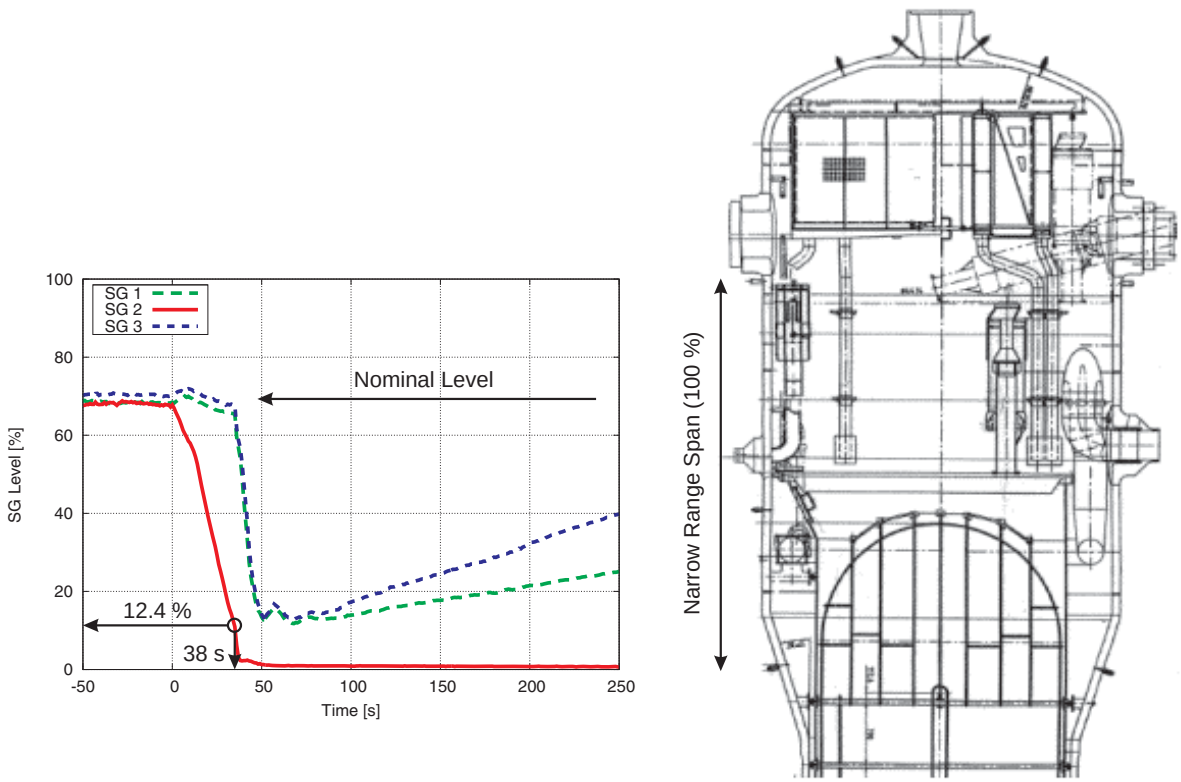

Figure 3 Narrow range levels in the upper part of SG 2

There are three pumps operating in the auxiliary FW system: two electrical pumps and one steam-driven pump. Each pump feeds one separate SG. The steam-driven pump delivers twice as much flow as the motor-driven ones, and it is connected to the steam generator three.

Shutting down of the reactor was followed by a turbine trip. Consequently, the pressure increased in the SG secondary side. With much less steam outflow, the temperature will also rise in the primary side. Therefore, the turbine bypass system actuates the steam dumping directly to the condenser in order to bring the temperatures back to normal.

The reactor SCRAM resulted in a radical decrease of the heat input to the primary side. The steam content of the SG secondary side started to drop. The auxiliary FW system provided the necessary amount of heat sink, which was adequate for removal of the residual heat and getting the SG levels back to normal. Finally, the plant was stabilized in a hot standby mode. All the systems behaved as postulated after the initiating event. The sequence of the main events is summarized in Table 1.

Table 1 Sequence of events during the transient

Time [s]	Event
0	FW control valve of SG-2 is closing due to malfunction
38	SG-2 level reached 12.4 % of narrow range: setpoint for SCRAM
38	Turbine control valve is closing
38	Auxiliary FW is actuated
39	Steam dump valve starts opening
47	Loop average temperature drops below 295 C
47	The intact SG-1 and SG-3 FW control valves start closing
77	Steam dump valves are closed
250	End of simulation

3. FEATURES OF THE RELAP5 MODEL

3.1 Status of the Model Development

The current model of Ringhals-3 was built on the basis of a legacy input created by Studsvik EcoSafe [3] for an earlier version of RELAP5 in 1994. Obviously, the RELAP5 code itself has gone through extensive changes during this period. Therefore, the model had to be thoroughly modified in order to comply with the syntax rules of the new code version, and to represent the current situation at Ringhals. But the most crucial goal was to provide a very detailed core description in accordance with a simultaneously developed neutron kinetic model for the PARCS code [4]. The code version used in this study is RELAP5/Mod3.3 Patch 3-hh, the latest version officially released under the CAMP user agreement at the time of preparation this document.

The majority of syntactical changes were related to the new volume and junction control flags, and the new connection coding requirements. The description of cross-flow junctions is easier and more logical with the application of the new expanded connection codes. Since the Henry-Fauske critical discharge flow model became the default option for the valve components in Mod 3.3, the corresponding valve parameters were updated accordingly.

The development of the model was carried out in successive steps. At first, the original structure of the cold leg, including the ECC mixer components were modified, following the explicit recommendations of the User's Guidelines [5]. Further structural changes were necessary on the secondary side. In order to capture the pressure pulse propagation, the number of sub-volumes of the steam line was increased by a factor of 10.

The largest modifications were related to the reactor pressure vessel internals. The initial model had a very coarse nodalization, including only one downcomer and two channels in the core. One "hot channel" represented the hottest fuel bundle, and one "average channel" represented all the rest of the active core. Therefore, the most significant refinement was done in the core region by modeling each of the 157 fuel assemblies individually, both for the hydrodynamics and for the heat structures. The main objective of the full radial description of the core is to study potential occurrence of asymmetric behavior during some certain transients. An attempt was made to apply as many axial nodes as available in the neutron kinetic calculation (altogether 24). However, this has exceeded the capacity of RELAP5. Consequently, the axial discretization of the active core was kept the same as in the old model, i.e. using 8 vertical nodes.

Results of the modeling studies have been summarized in various conference papers and technical reports [6], [7], [8], [9], [10], [11], [12], [13].

3.2 Description of the Nodalization

The RELAP5 nodalization schemes of the reactor pressure vessel (RPV) internals and the primary side are depicted in Figure 4 and Figure 5, respectively. Description of the most important parts of the model is given in the followings. The referenced component numbers appear in parentheses.

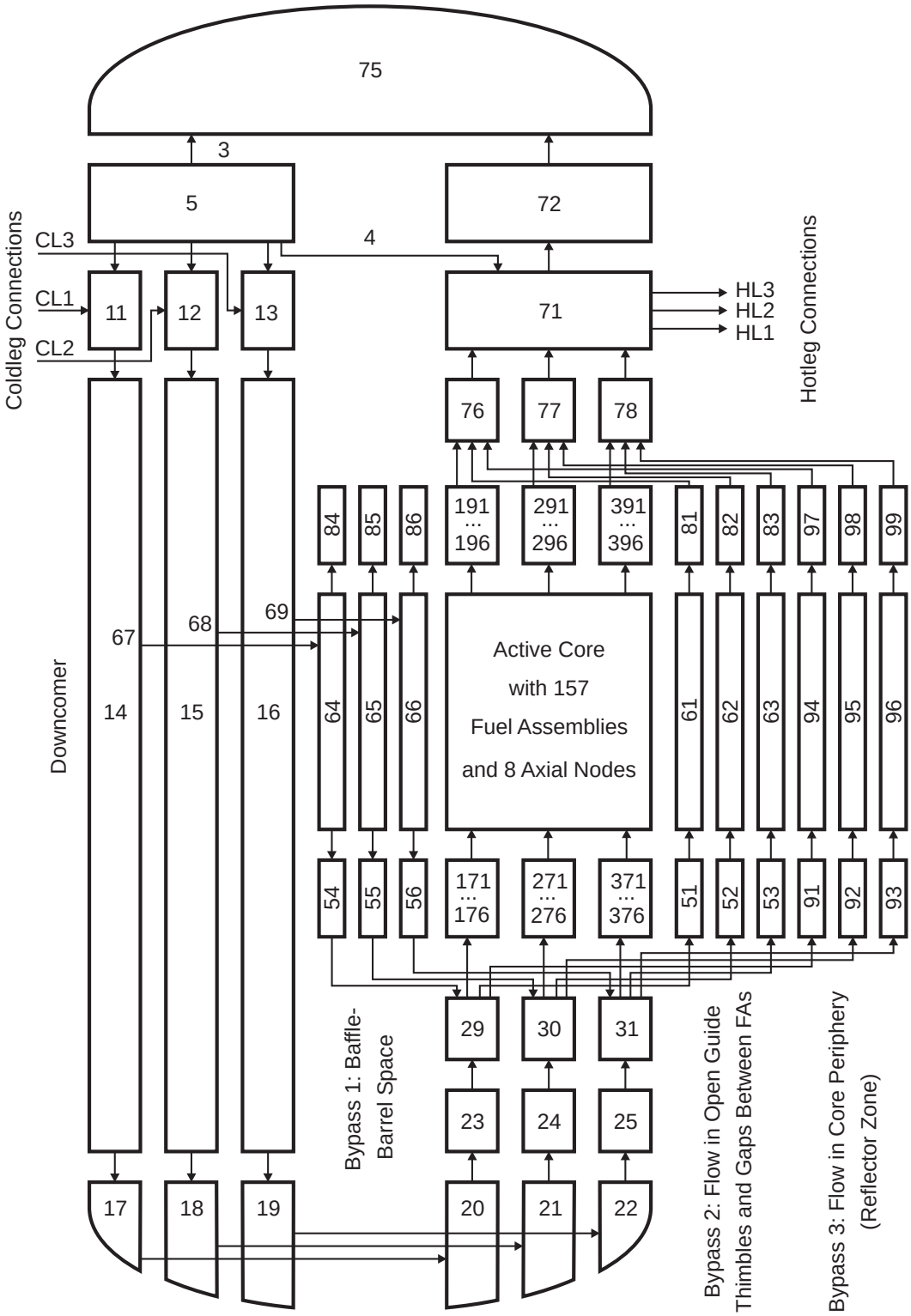

Figure 4 Nodalization of the reactor pressure vessel internals

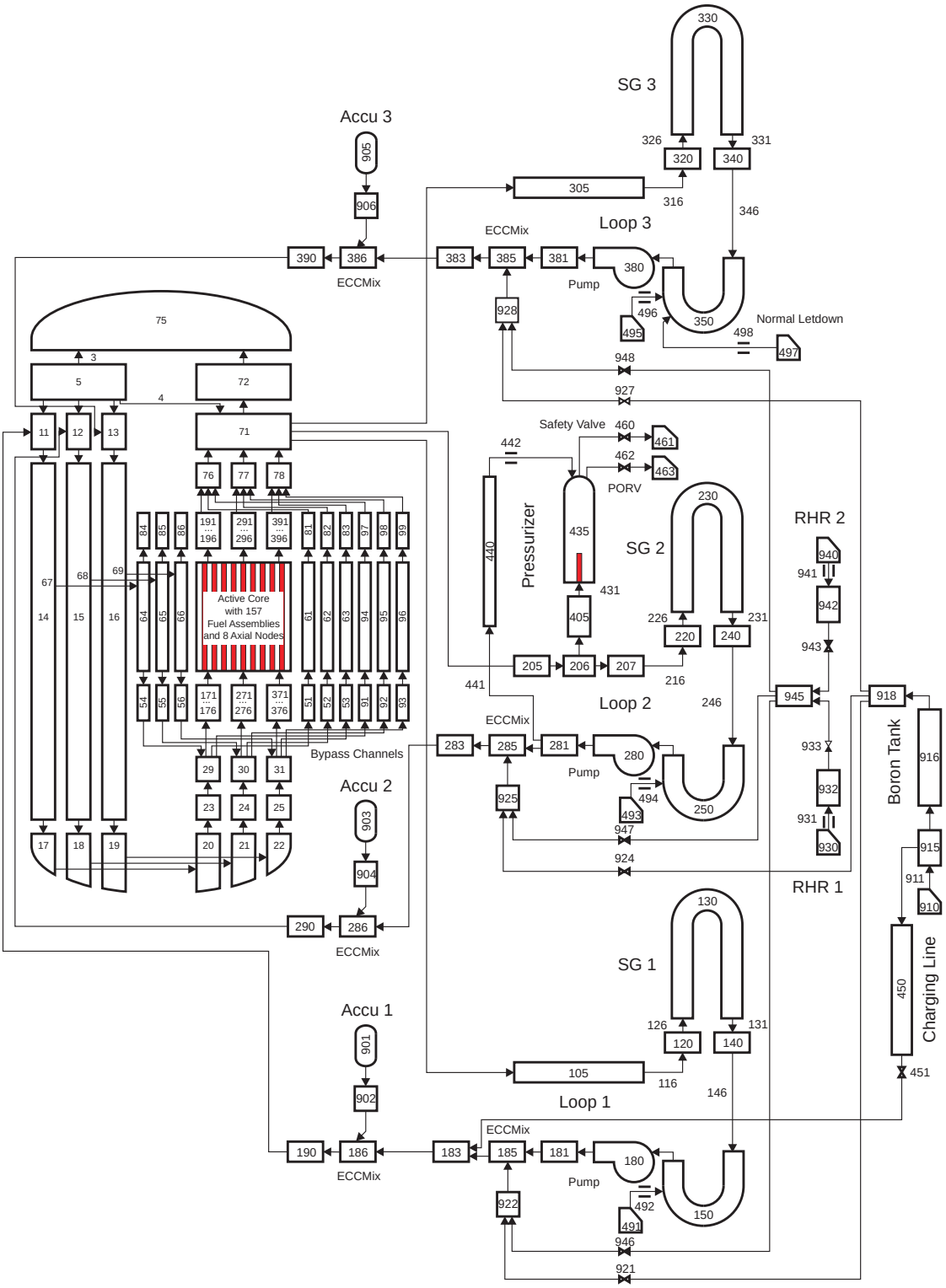

Figure 5 Nodalization of the primary side

3.2.1 The downcomer

It is essential that some specific phenomena, for instance an asymmetric behavior of the loops should be captured properly. For this reason, the downcomer and the core were split into 3 parallel channels in order to retain the 3-loop structure of the primary side even within the reactor pressure vessel. The coldlegs are connected to the top of the downcomer via branches 011, 012, and 013. The downcomer is modeled with 3 annulus components (014, 015, and 016) representing 1/3 of the total flow area, each divided into 6 axial volumes.

3.2.2 The lower plenum

The large volume at the bottom of the RPV is modeled with altogether 6 volumes, 3 out of them representing the down-flow region (017, 18, and 019) and the other 3 represent the upwards flow part (020, 021, and 022).

3.2.3 The core inlet

The bottom of the core region consists of the lower support plate, the bottom nozzle, and the core plate models (23…28). The core inlet and outlet needed special considerations due to a limitation in RELAP5, since a branch component may be connected to maximally 9 other volumes from its each face. Thus, arrangement of 157 junctions to the fuel assemblies was realized by application of altogether 18 branches (171…76, 271…276 and 371…376).

3.2.4 The core

From hydrodynamic point of view, the fuel assemblies are modeled with vertical pipe components, axially divided into 8 volumes. It is assumed that 52 channels belong to one radial “sector” of the core (Figure 6). One loop is associated with one radial sector, i.e. 1/3 of the core. The fuel assembly models are basically identical, except the channel at the centre of the core (364).

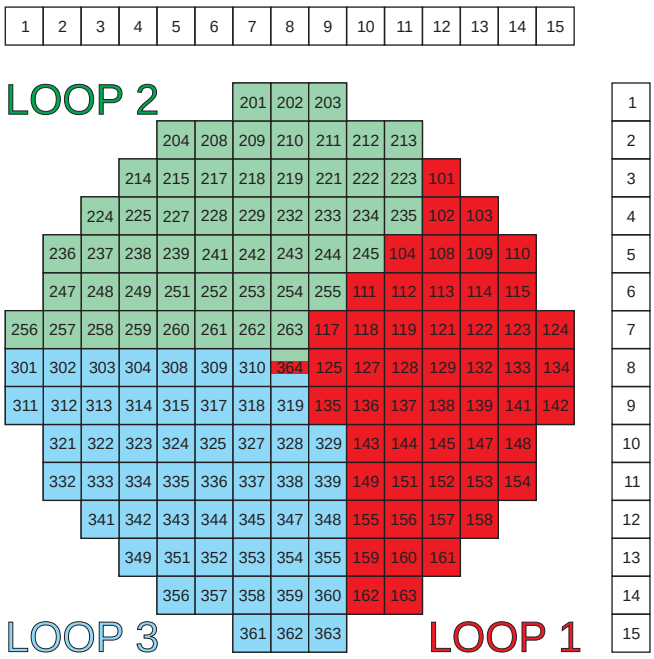

Figure 6 Numbering scheme of the fuel channels in radial sectors

A fuel assembly is modeled with a heated channel. The heat source of the fuel rod is provided by either a control variable (in a stand-alone RELAP5 calculation), or by the neutron kinetic code (in a coupled RELAP5/PARCS simulation). A fuel element has 9 radial mesh points. Locations and the material compositions are shown in Figure 7. The relative axial power distribution is approached by a curve shown in Figure 8.

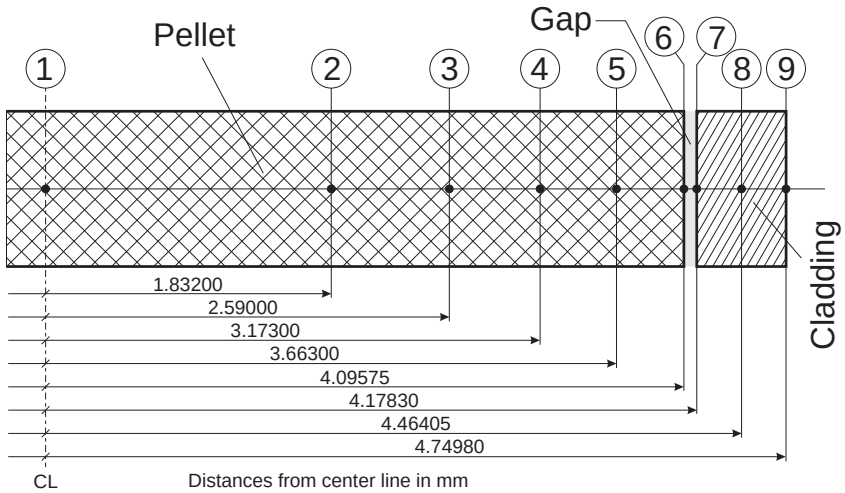

Figure 7 Radial mesh points and material compositions in the fuel elements

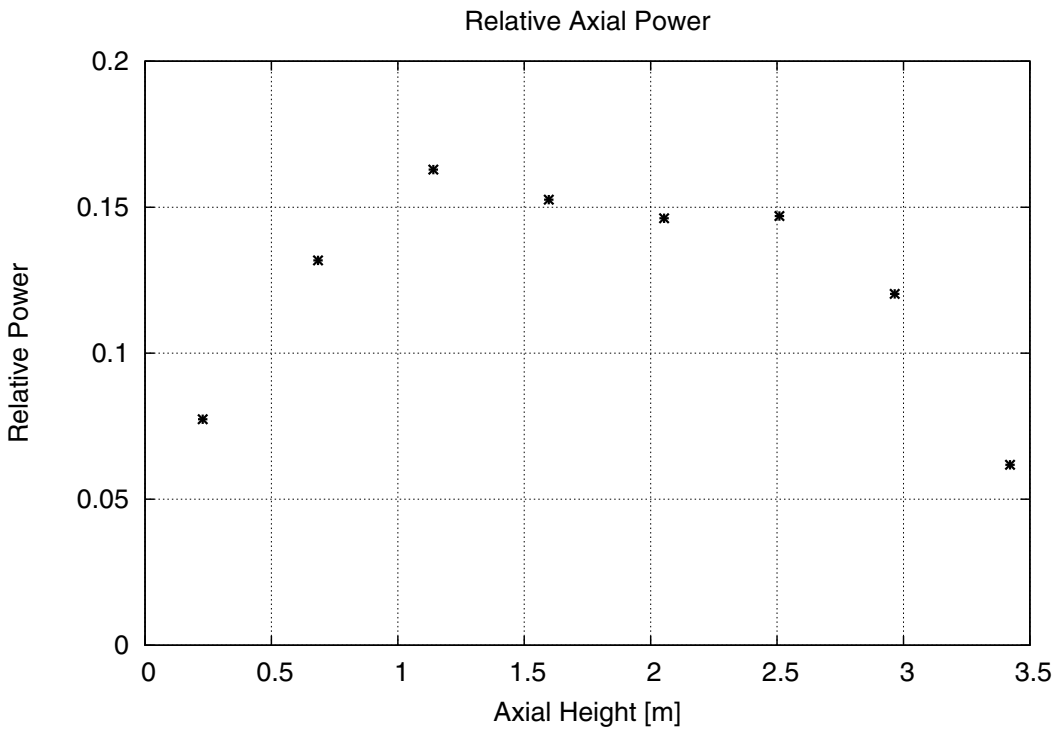

Figure 8 Relative axial power distribution

3.2.5 The bypass channels

It is also important to distinguish between the coolant flowing through the fuel assemblies while being heated, and the remaining part of the main loop flow. Thus, the core has been extended with altogether 3 bypass channels per loop, representing

- the *unheated baffle-barrel space*,
- the *open guide thimbles*, and
- the flow path at the *core periphery*

The latter one is associated with the reflector zone explicitly modeled in the neutron kinetic code. The total amount of bypass flow was found to be playing an important role in the over-all core heat transfer. Consequently, the hydrodynamic parameters were carefully set in order to reproduce the measured ratio between the main flow and the bypass flow. Locations of the grid spacers were taken into account at setting the flow resistances and loss coefficients in the fuel bundle. Compared with plant data, these efforts resulted in a realistic pressure loss distribution over the core.

3.2.6 The upper plenum

The upper, inactive part of the core is simulated with 18 additional branch components in a similar manner as of the core inlet. The upper plenum consists of the core exit volumes (191…196, 291…296 and 391…396) branching into 3 volumes (76, 77 and 78). The hot legs are connected to volume 71. The top of the RPV is modeled with a large volume (75).

3.2.7 The hot and cold legs

Loop 1 and loop 3 are essentially similar, while loop 2 is somewhat different because of the pressurizer. The length of the hot leg between the RPV outlet and SG inlet nozzle is L = 5.438 m, with an inner diameter of D = 0.7366 m. The length of the cross-over leg between the SG outlet and the pump inlet is L = 6.715 m, the diameter is D = 0.7873 m. The corresponding data for the cold leg (between the pump outlet and RPV inlet nozzle) are L = 7.331 m and D = 0.6985 m, respectively.

3.2.8 The pressurizer

The PRZ is modeled with 12 internal volumes in a pipe component (435). The lower 3 volumes are associated with electric heaters. The PORV (462), a safety valve (460), and the injection line of the PRZ spray system (440) are connected to the top volume of the PRZ. The mass flowrate of the sprayed coolant is controlled by a time dependent junction (442). The surge line (405) is branching from the cold leg (205) and it is connected to the bottom of the PRZ.

Due to similarity of the 3 loops, the numbering scheme of the components is analogous within loop 1, 2, and 3. Thus, x denotes 1, 2, or 3 in the following description of the components, respectively.

3.2.9 The SG primary side

The primary fluid enters the SG at the inlet nozzle and plenum (x20), consisting of 5 internal volumes. The vertical bundle of the heat exchanger tubes are modeled with one characteristic pipe (x30). Both legs of the U-tubes are partitioned into 13 vertical sub-volumes. The top of the bundle is represented by one horizontal sub-volume. The outlet plenum (x40) is symmetrical to the inlet.

3.2.10 The main circulation pumps

The MCPs are modeled with pump components. The homologous curves, torque and head data were obtained from plant documentation. The model was not modified in the new version of the input deck.

3.2.11 The safety systems

One hydro-accumulator component (901, 903, and 905) is connected to each loop of the primary system through an emergency core cooling mixer component (x86). These ECC mixers are operating in tandem with the other mixers (x85) that may inject water either from the boron tank (916) or from the residual heat removal system (930 and 940).

The primary side model is extended with a time dependent junction (498) simulating the normal letdown, and a charging line (450) and the corresponding valve (451).

3.2.12 The feedwater system

The boundary conditions for the normal feedwater are set in a time dependent volume (581). Distribution of the FW takes place in a branch component (854). The normal FW line consists of a control valve (862, 872, and 882) and an isolation valve (864, 874, and 884), respectively in each loop. The auxiliary FW is taken from the boundary volumes (891, 893, and 895). The mass flowrate of the injected auxiliary FW is controlled by time dependent junctions (892, 894, and 896).

3.2.13 The Steam Generators

The nodalization of the secondary side is shown in Figure 9. Similarities of the loops are utilized also in the case of numbering scheme of the SGs. Therefore, the internal structural elements of SG-1, 2, and 3 are denoted with component numbers 5xx, 6xx, and 7xx, respectively.

The FW enters to the SG at a branch (x76). The downcomer is modeled with a pipe component (x80) split into 5 vertical volumes. The large boiler section (x05) has altogether 14 axial volumes with internal diameter of 3.105 m.

The tube support grids are taken into account. The bundle interphase friction model is applied in this region. Separation of the steam takes place in a separator component (x40). The inlet, the outlet and the liquid fallback junctions are connected to appropriate branch components (x35, x50, and x72, respectively). A steam dryer (x55) is situated in the upper part of the SG.

3.2.14 The Steam Line

The steam line is split into 2 parts (x85 and x95), each partitioned to 10 volumes. The main steam isolation valve (x94) is connecting the 2 parts together. Relatively high resolution of meshing was chosen in order to capture propagation of pressure pulses along the steam lines. Altogether 6 safety valves (x86…x91) and a relief valve (x92) are connected to the steam line, in parallel with each other.

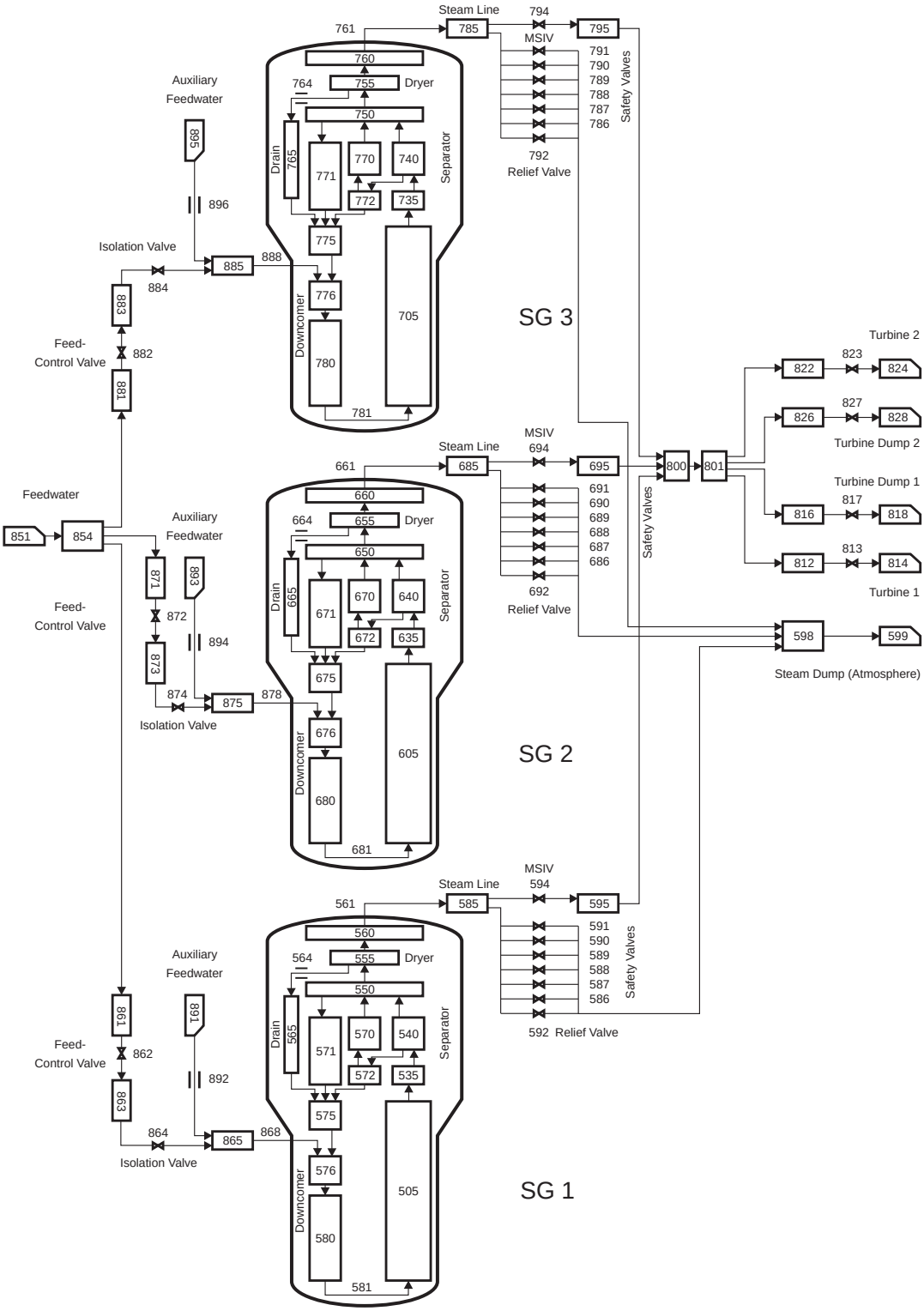

Figure 9 Nodalization of the secondary side

3.2.15 Turbines and steam dump systems

The steam lines are merging at a branch component (800). The Ringhals-3 unit has 2 turbines and 4 turbine dumps. These components are modeled in a simplified way in the current RELAP5 model. Turbine 1 and 2, and their control valves are simulated with time dependent junctions (814 and 824) and motor valves (813 and 823), respectively. One turbine dump system model is a combination of 2 real dump systems in the plant (time dependent volumes 818 and 828).

The control and protection systems were designed carefully and the parameters strictly follow the values laid out in the Ringhals-3 PLS document [14]. Improvement in the modeling of the control system resulted in a more realistic simulation of the feedwater flow by controlling the speed of the feedwater pumps. The controls influencing the steam dump system was also updated on the basis of new specifications.

4. RESULTS OF THE BASE CASE CALCULATIONS

4.1 Reaching steady-state

The steady-state initialization took approximately 300 s, running the codes with “transient” option on card 100. Using this option instead of “steady-state” was necessary in order to avoid a premature termination of the calculation. (Earlier test-runs resulted in false indications of reaching steady-state, in spite of some key parameters were in fact varying).

The following strategy was applied in for achieving steady-state. The calculated heat balance resulted in a particular primary loop flowrate. This mass flowrate was set as the prescribed quantity for the circulation pumps to be reached by variation of the pump speed. The level in the PRZ was achieved by letting the PRZ spray and heaters to be actuated according to their real control systems. On the secondary side, the necessary SG level was reached by controlling the feedwater flow.

In order to demonstrate the steady-state search process by the computer code, the main characteristic parameters are plotted on the next few pages.

Due to the pump speed control system, the primary side loop flowrate (Figure 10) stabilized very rapidly. Only relative value of this parameter was available in the measured database. Therefore, the corresponding numerical value (expressed in kg/s, instead of %) was determined from the heat balance.

The level control system of the SGs regulated the amount of feedwater (Figure 11) and steam (Figure 12). As it can be seen in these figures, the stabilized values converged to approx. 492 kg/s. Due to loop asymmetry, the injected FW to SG-2 is approx. 1 kg/s higher. Minor discrepancy (less than 3 %) was found between the measured and calculated steady-state values of the FW. Nevertheless, this can be explained by the precursory event of the control valve malfunctioning before the transient initiation, which is not part of the steady-state simulation.

Basically, identical amounts of FW and steam mass flow rates led to stable levels in the SGs. As Figure 13 indicates, the narrow range SG levels converged to approx. 69 %, and this value is in very good agreement with the measured data.

Secondary side pressures are depicted in Figure 14. The stationary pressures approached the measured value with a good accuracy. Concerning SG-2, a minor asymmetry is naturally present also in this case.

The primary system pressure is maintained by a boundary volume connected to the PRZ. It can be observed in Figure 15 that the necessary pressure is assured by this arrangement. Obviously, the boundary volume is eliminated at the transient initiation.

Both the cold leg (Figure 16) and hot leg (Figure 17) temperatures stabilized exactly at their measured values. Thus, it can be concluded that the over-all calculated parameters became stable and reflected the measured plant data with a good degree of accuracy at the end of the current initialization process. Numerical values are summarized in Table 2.

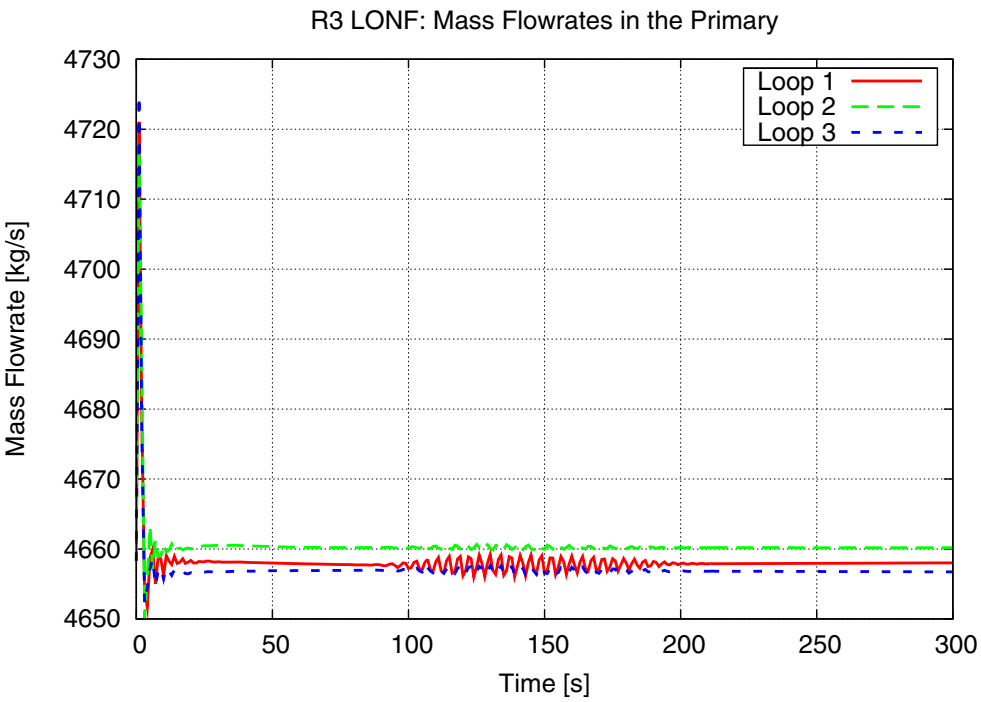

Figure 10 Steady-state search of primary loop flowrate

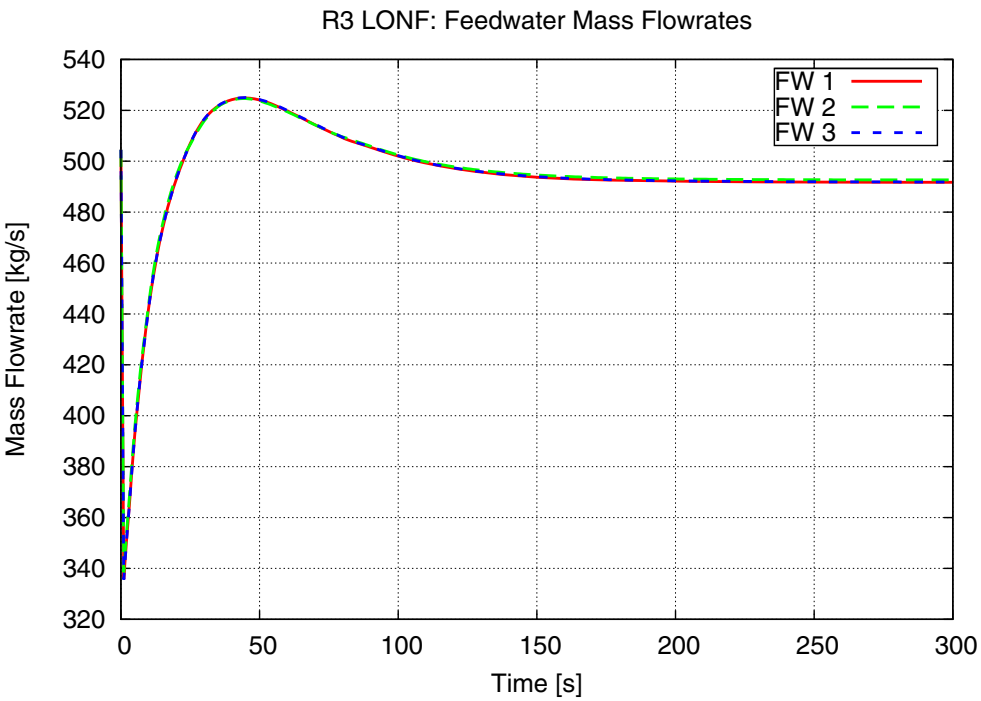

Figure 11 Steady-state search of feedwater mass flowrate

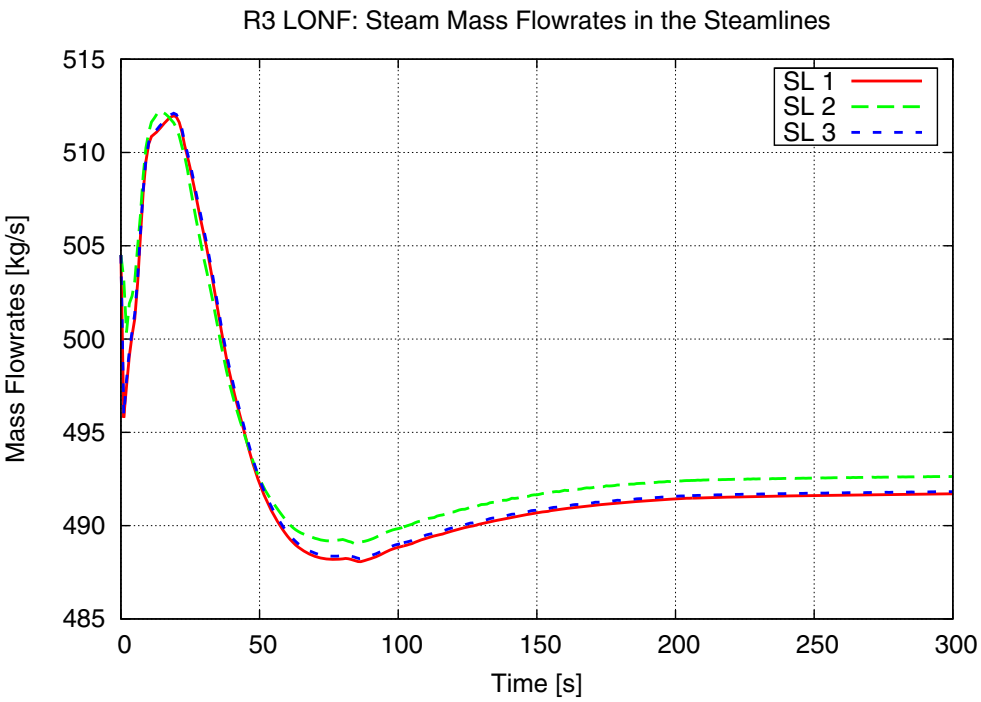

Figure 12 Steady-state search of steam mass flowrate

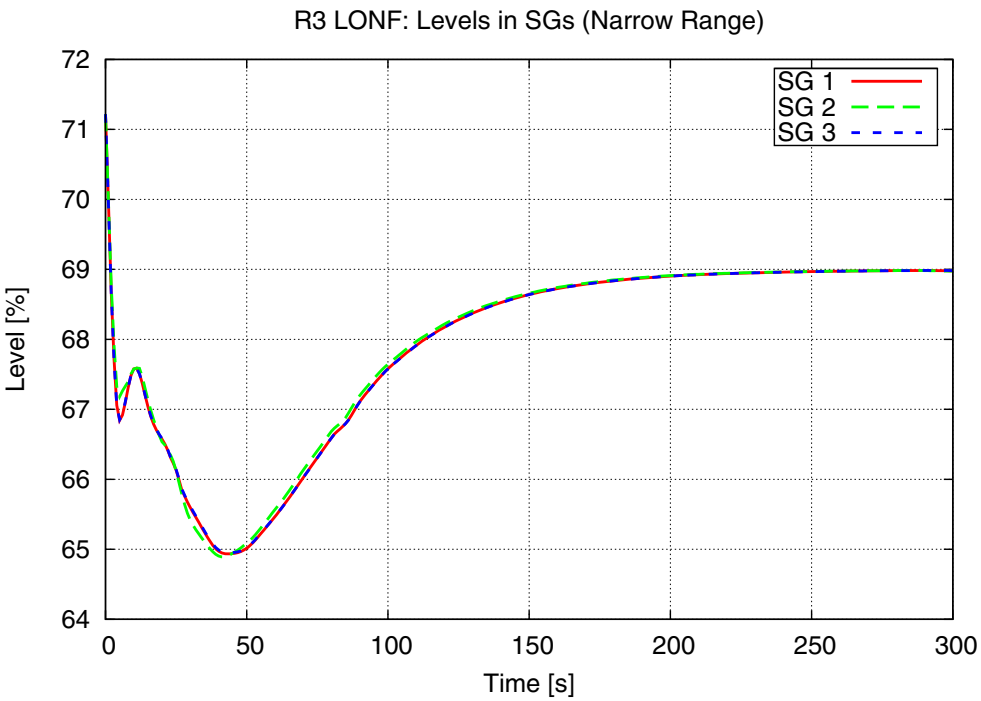

Figure 13 Steady-state search of narrow range SG level

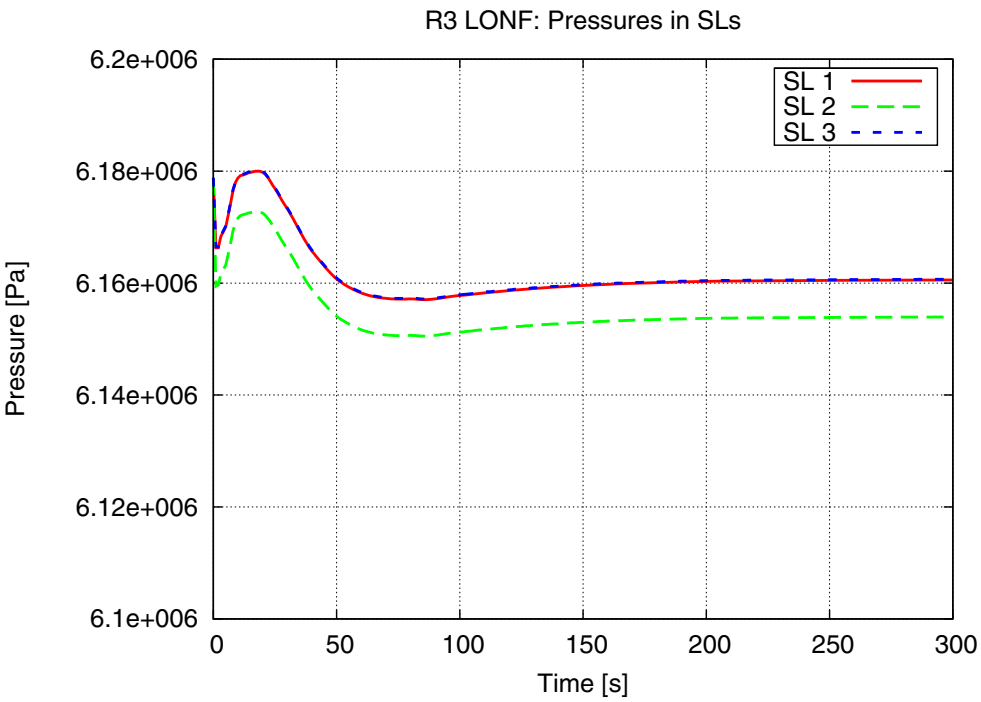

Figure 14 Steady-state search of pressures in the steam line

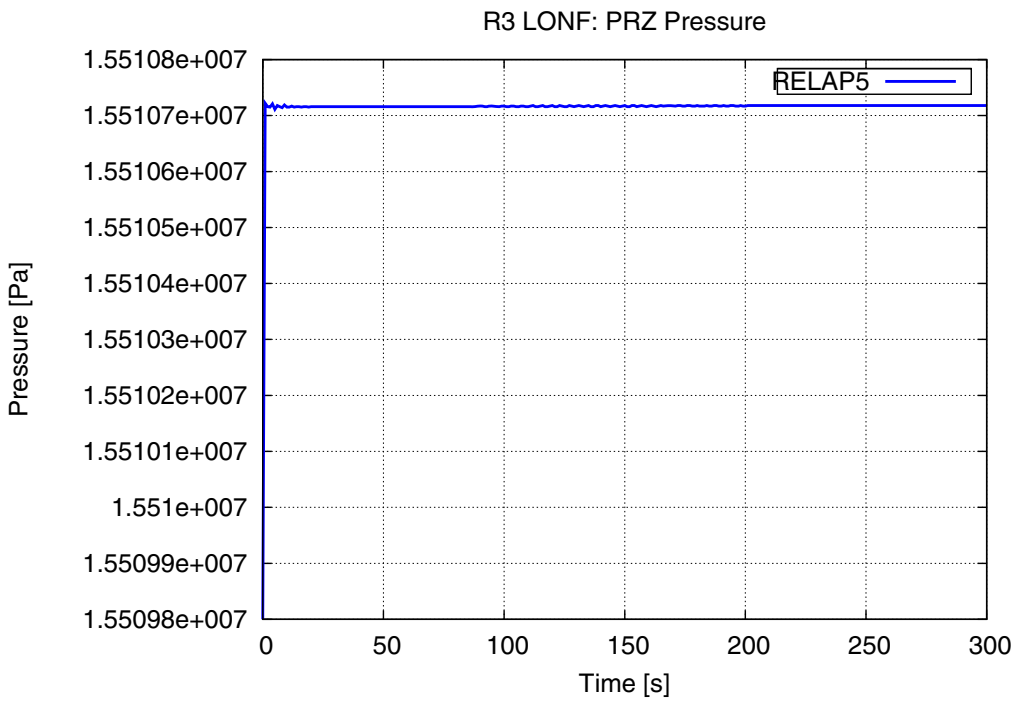

Figure 15 Steady-state PRZ pressure provided by a boundary volume

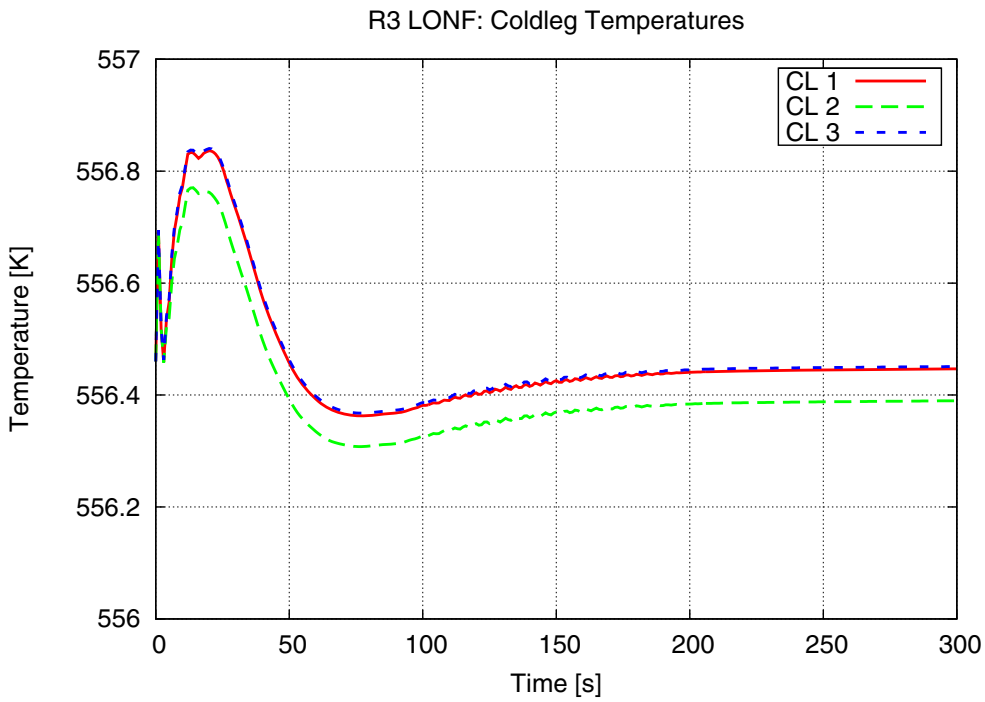

Figure 16 Steady-state search of coldleg temperatures

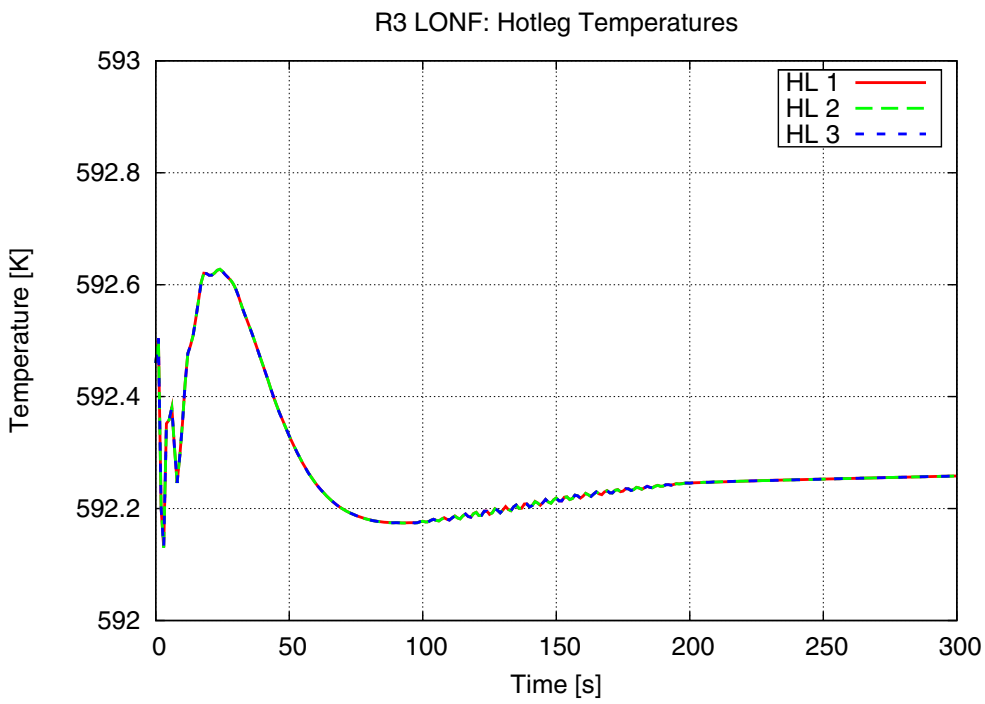

Figure 17 Steady-state search of hotleg temperatures

Table 2 Comparison of calculated and measured steady-state parameters

Parameter	Name in RELAP5	Unit	Steady-state value	RELAP5 average	Measured average	Deviation [%]
Mass flow in loop 1	mflowj-180010000	kg/s	4658.01	4658.30	4654.12*	0.0898
Mass flow in loop 2	mflowj-280010000	kg/s	4660.17			
Mass flow in loop 3	mflowj-380010000	kg/s	4656.73			
FW flowrate to SG 1	mflowj-868000000	kg/s	491.75	492.10	507.21	2.9796
FW flowrate to SG 2	mflowj-878000000	kg/s	492.70			
FW flowrate to SG 3	mflowj-888000000	kg/s	491.85			
Steam flowrate in SL 1	mflowj-594000000	kg/s	491.70	492.05	507.88	3.1171
Steam flowrate in SL 2	mflowj-694000000	kg/s	492.64			
Steam flowrate in SL 3	mflowj-794000000	kg/s	491.82			
Level in PRZ	cntrlvar-430	%	43.49	43.49	43.24	0.5692
NR level in SG 1	cntrlvar-521	%	68.98	68.98	68.96	0.0268
NR level in SG 2	cntrlvar-621	%	68.98			
NR level in SG 3	cntrlvar-721	%	68.98			
Normalized power	cntrlvar-002	-	1.00	1.00	1.00	0.00
Pressure in PRZ	p-435120000	Pa	15510718	15510718	15506794	0.0253
Pressure in SL 1	p-585050000	Pa	6160558	6158397	6165568	0.1163
Pressure in SL 2	p-685050000	Pa	6153947			
Pressure in SL 3	p-785050000	Pa	6160688			
Temperature in CL 1	tempf-181010000	K	556.45	556.43	556.45	0.0029
Temperature in CL 2	tempf-281010000	K	556.39			
Temperature in CL 3	tempf-381010000	K	556.45			
Temperature in HL 1	tempf-105030000	K	592.26	592.31	592.54	0.0382
Temperature in HL 2	tempf-205030000	K	592.42			
Temperature in HL 3	tempf-305030000	K	592.26			

* From heat balance calculation

4.2 Transient results

As it was mentioned in the Introduction, the relevant transient started with malfunctioning of the guiding electronics of the FW control valve in the injection line connected to SG-2. The amount of FW flow deviated from its stable value about a minute prior to the eventual shut down of the valve. This precursory event appears as an oscillation in Figure 18. Since this period was not part of the transient simulation, the FW mass flowrate was approximated with its average steady-state value. The transient began with an instant loss of FW, which was modeled with a prompt closure of valve in the code.

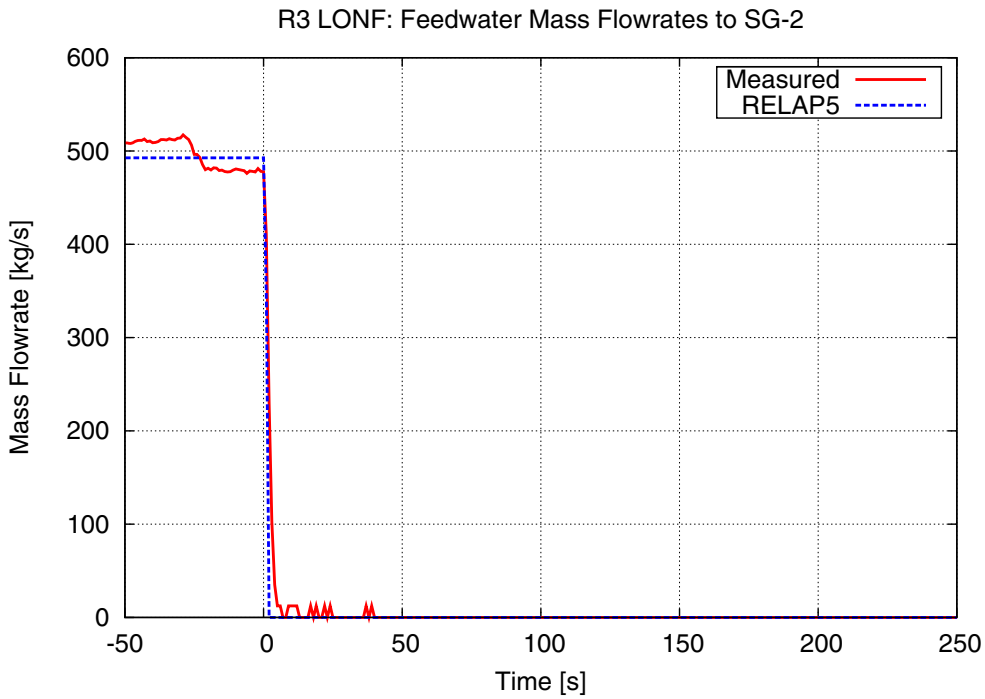

Figure 18 Feedwater mass flowrate to the malfunctioning SG-2

Sinking of the level started immediately as it can be seen in Figure 19, reaching the so-called "*Low-Low Level*" reactor trip condition at approx. 34 s. The narrow range measurement supplies higher resolution data, however, it obviously indicates zero value when the level passes below its lower differential pressure transducer. Hence, the wide range measured data are more suitable for comparison after the reactor SCRAM (Figure 20).

The code was able to reproduce almost the entire period of level decrease. Dropping of the level stopped at approx. 35 % of wide range data and was followed by a slow increase. However, regaining of the level took place with a lower gradient than in the measurement. This was partly due to the underestimated amount of AFW injected to SG-2, as will be explained later on, and it is also a subject of a parametric study.

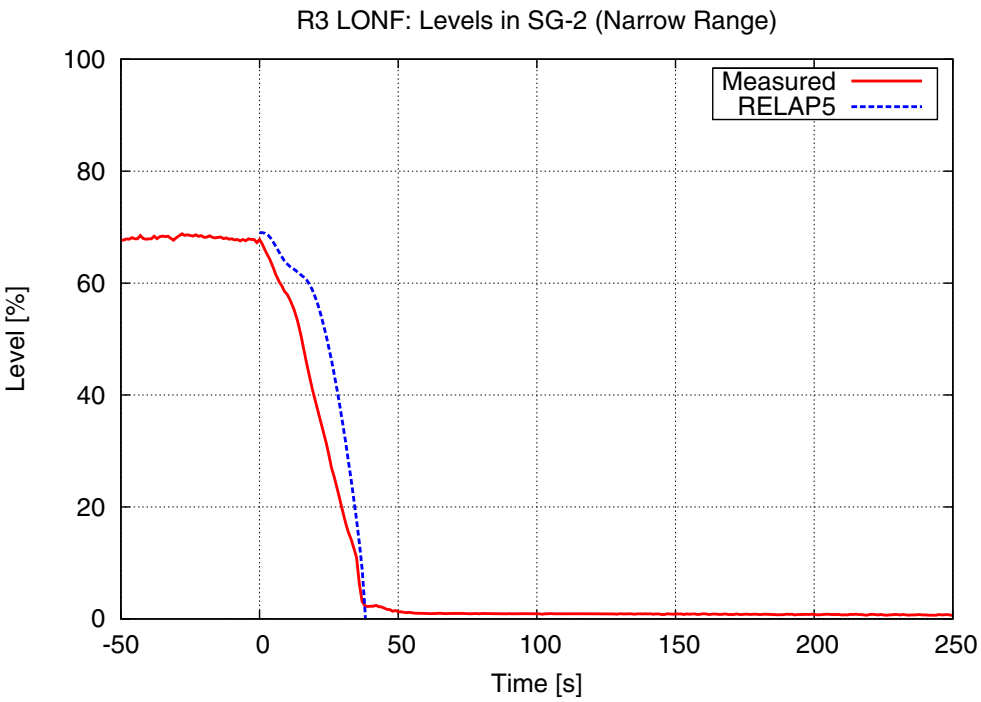

Figure 19 Narrow range level in the malfunctioning SG-2

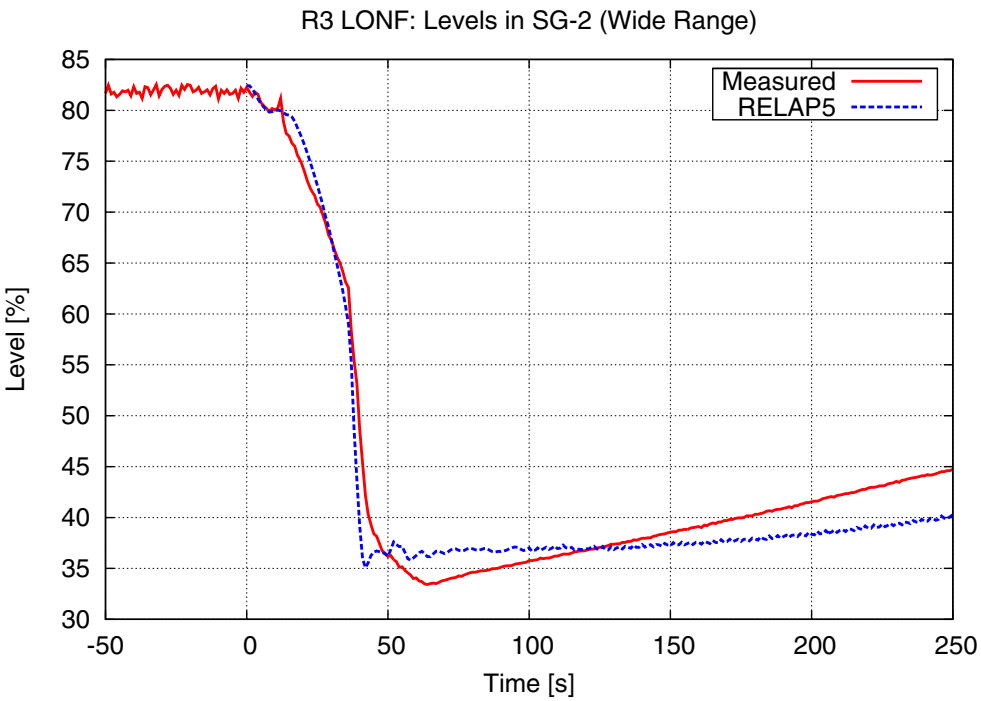

Figure 20 Wide range level in the malfunctioning SG-2

Because of reaching the *"Low-Low Level"* condition, the reactor was tripped. Most importantly, the code was able to capture the timing of the SCRAM signal. Concerning the reactor power, the measurement comes from power range monitoring ex-core detectors calibrated against calorimetric measurements at relatively large power levels. Such a calibration does not hold for low power levels, as the ones monitored after a reactor SCRAM (decay heat), thus explaining why the best approach was found to be simulating the decay heat curve with a boundary condition according to the well-established ANS-5.1 standard.

Figure 21 shows the values of the relative power. The measured data represent the average of 4 neutron flux transducers located at the same azimuth around the core but at two different axial elevations. The RELAP5 curve indicates also the relative amount of residual heat in the core after the SCRAM, with respect to the steady-state value.

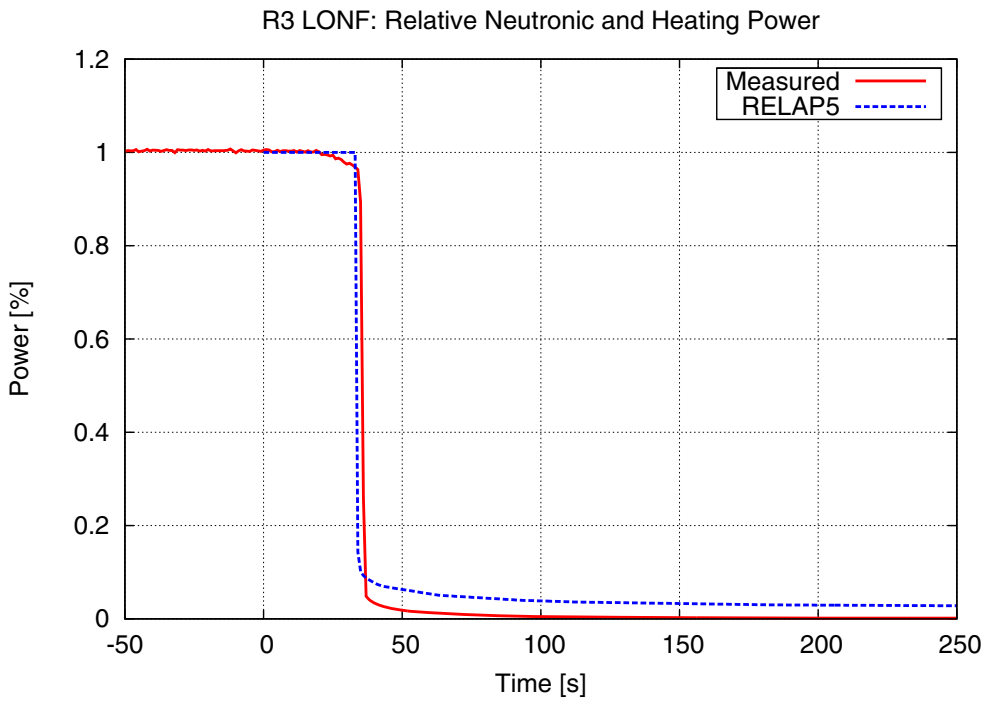

Figure 21 The measured neutronic power and the relative heating power

Variation of the pressures in the (intact) SG-1 is depicted in Figure 22. Matching of the measured and simulated data is excellent. A small discrepancy can be observed soon after the initiation of the transient. Increase of the pressure took place in the secondary side when the turbine throttle control valves started to close to maintain the nominal power. Since the full turbine system, including the unknown throttling valve characteristics, is modeled in a simplified way, the pressure data are slightly different during a short interval between 15 and 37 s.

Simulation of the pressure has been achieved with a same degree of accuracy in the malfunctioning SG-2. The code managed to reproduce the sudden increase of the pressure during the closure of the turbines, followed by dumping of steam into the condenser (Figure 23).

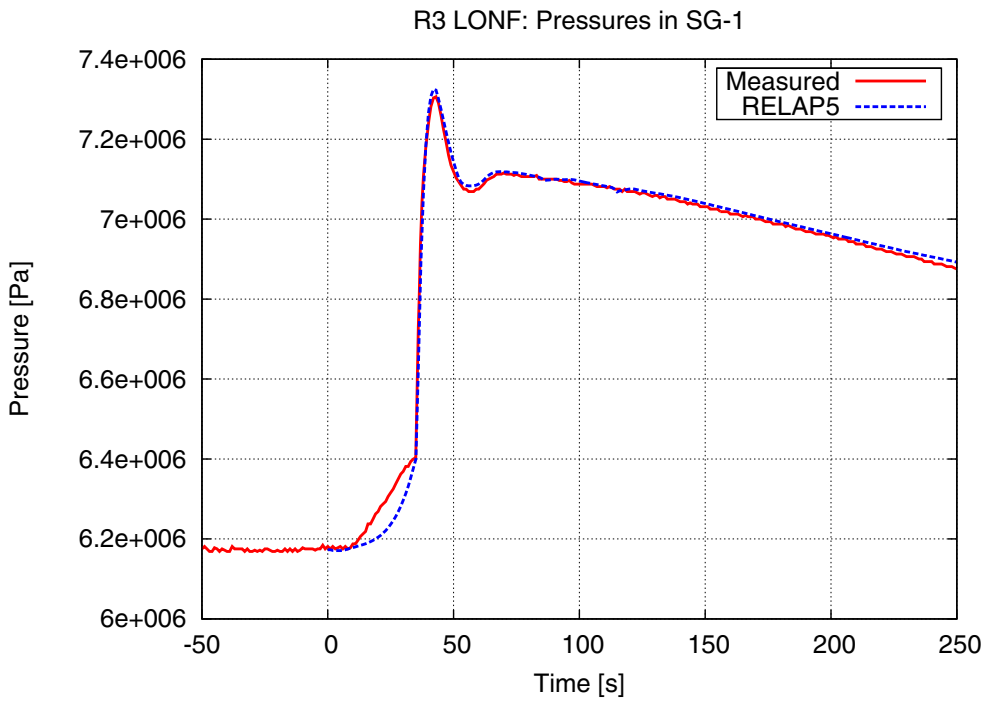

Figure 22 Pressure in the intact SG-1

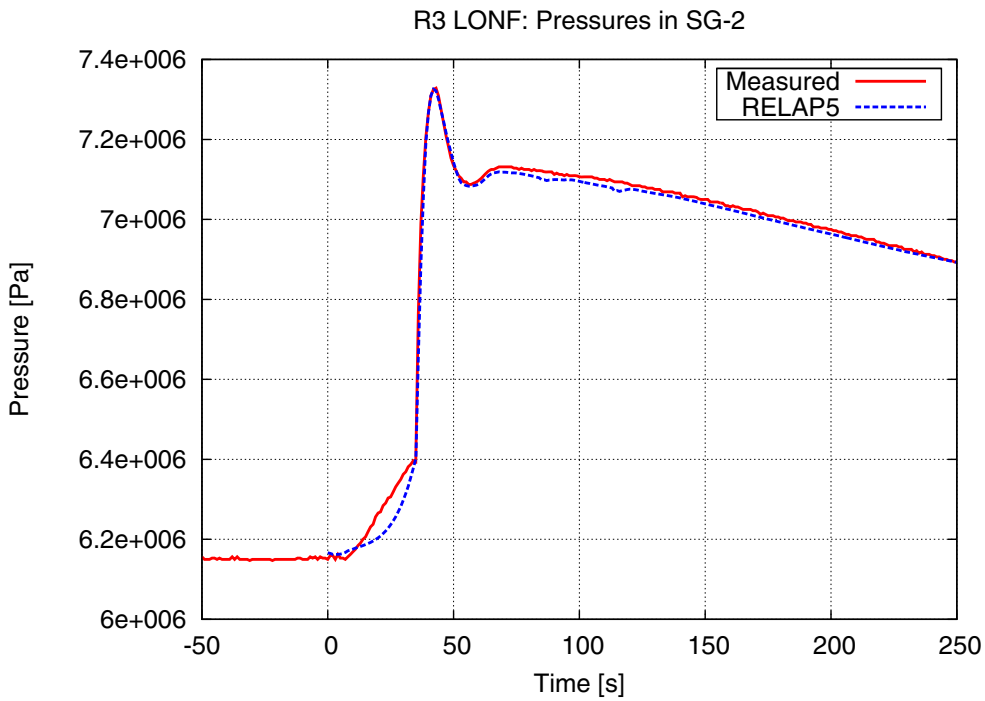

Figure 23 Pressure in the malfunctioning SG-2

Response of the system to such a large disturbance can induce asymmetric behavior in the loops. One example for such differences is the amount of steam produced by steam generators. The mass flowrate in steamline 1 is shown in Figure 24.

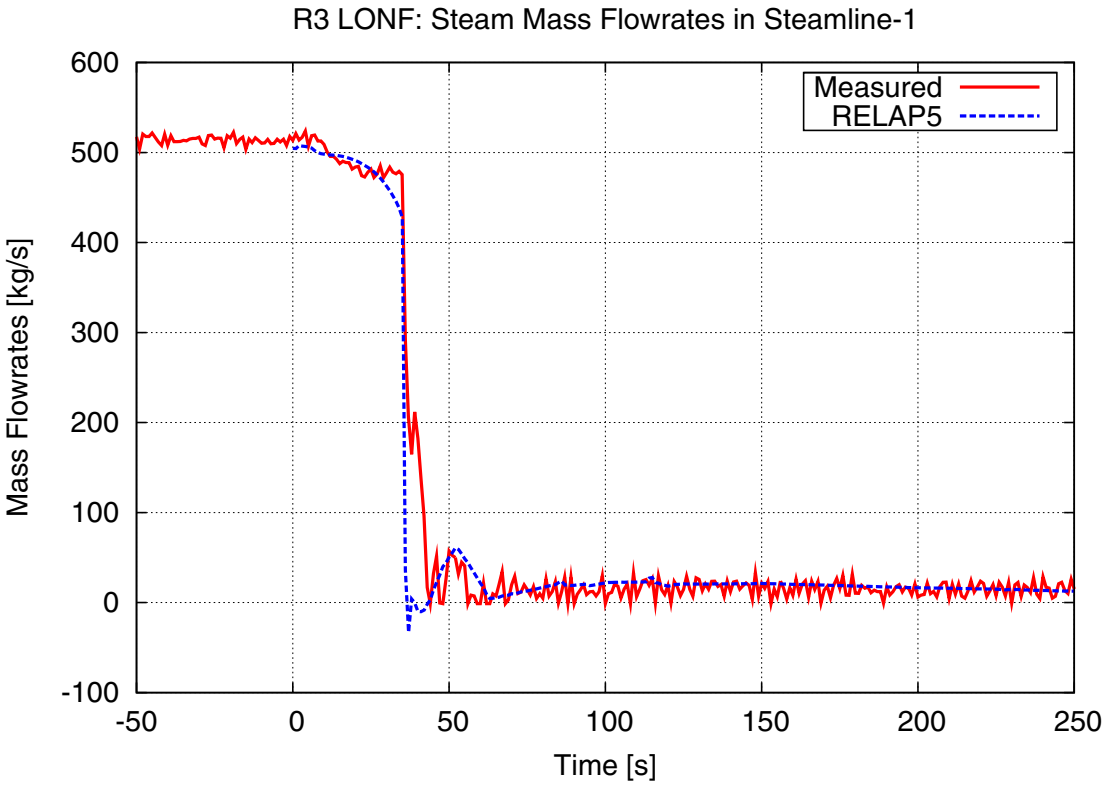

Figure 24 Steam mass flowrate in steamline 1

The steam flow started to decrease from the intact SG-1 soon after the transient initiation, reaching a value of approx. 480 kg/s. Just around the time of the reactor SCRAM, the steam production was reduced almost instantaneously. This was interrupted by a small increase a few seconds later and followed by a continued dropping. The simulation could not reproduce this phenomenon, but instead it calculated a monotonous decrease, down to a minimal amount of steam.

Opening of the steam dump valves resulted in a minor increase of the mass flowrate in the steamlines at around 50 s. This was also captured by the code, as well as the small amount of steady flow for the rest of the transient.

Oscillatory nature of the measured steam flow is probably owing to the fact that the flow measurement system is not calibrated for such a small amount (5 – 7 %) of the nominal steam mass flowrate in the final phase of the transient.

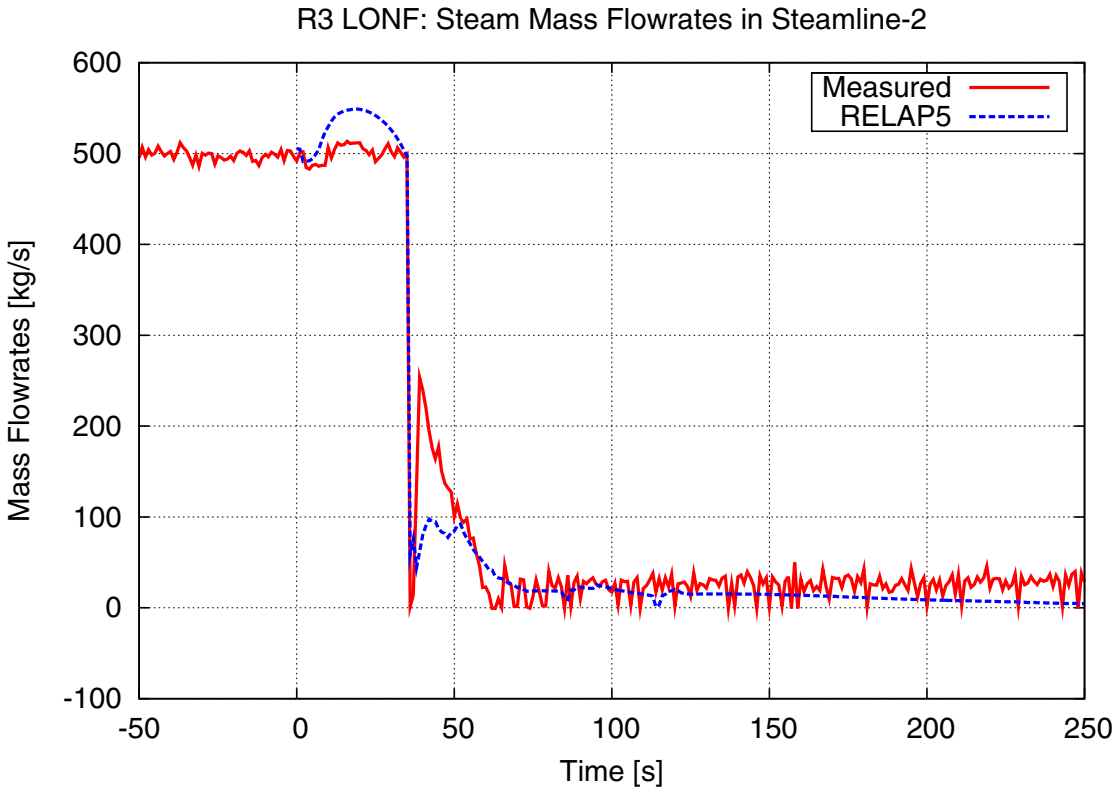

Figure 25 Steam mass flowrate in steamline 2

In the case of the malfunctioning SG-2, the amount of steam was initially increasing due to the total lack of FW injection. This phenomenon was present in the calculation but RELAP5 overestimated the flowrate, reaching the maximum of approx. 550 kg/s. Nevertheless, timing of the sudden closure of the control valve was perfectly matched. The intermittent dump valve opening resulted in a peak mass flowrate above 200 kg/s. The code calculated half as much steam dumped to the condenser during this short period. This is an indication for necessity of further improvement of the steam dump control system in the model.

Concerning the collapsed levels in the other two intact steam generators, performance of the code is sufficiently good (Figure 26 and Figure 27). The narrow range measurements were available for the whole duration of the transient in this respect, since the levels were maintained above the lower taps of the differential pressure transducers.

The dynamic response of secondary side is really good until approx. 100 s for both of the intact SGs. Lower speed of the level increase may be an indication of underestimated amount of auxiliary FW. This theory was supported when the available measured database and the plant documentation were compared. According to the latter one, the capacity of the turbine-driven AFW pump is approx. 48 kg/s. On the contrary, the measured AFW flow signal showed “saturation” when it approached 30 kg/s. In order to rectify this possible measurement flaw, the nominal value of the AFW mass flowrate (i.e. 48 kg/s) was used throughout the calculation. However, even this higher flowrate was found to be inadequately low for reproducing the correct SG levels.

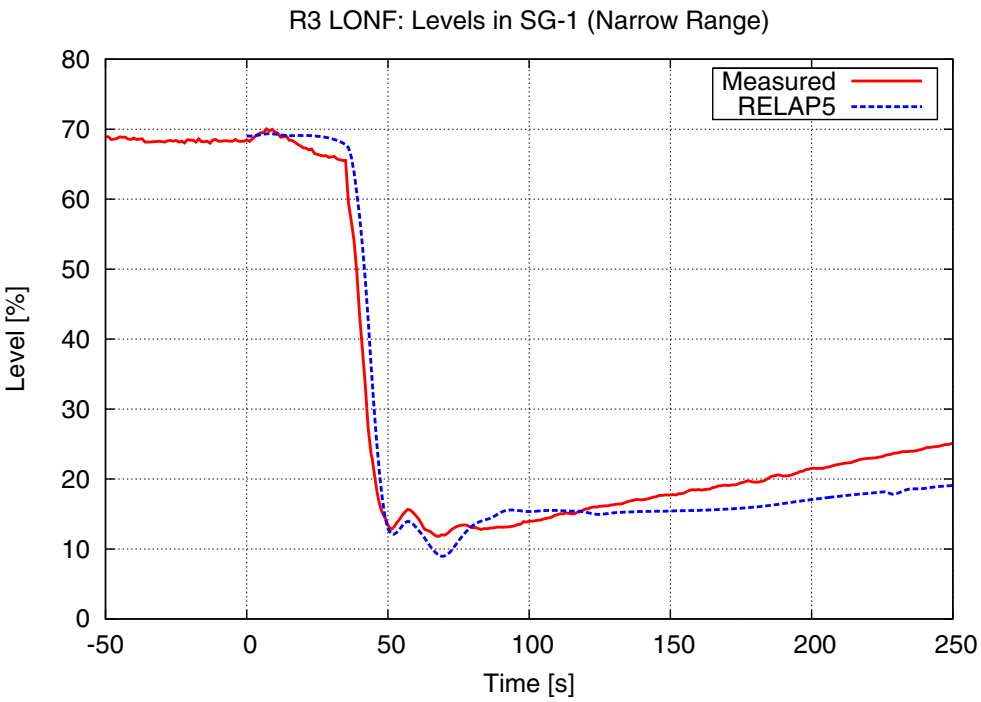

Figure 26 Narrow range level in the intact SG-1

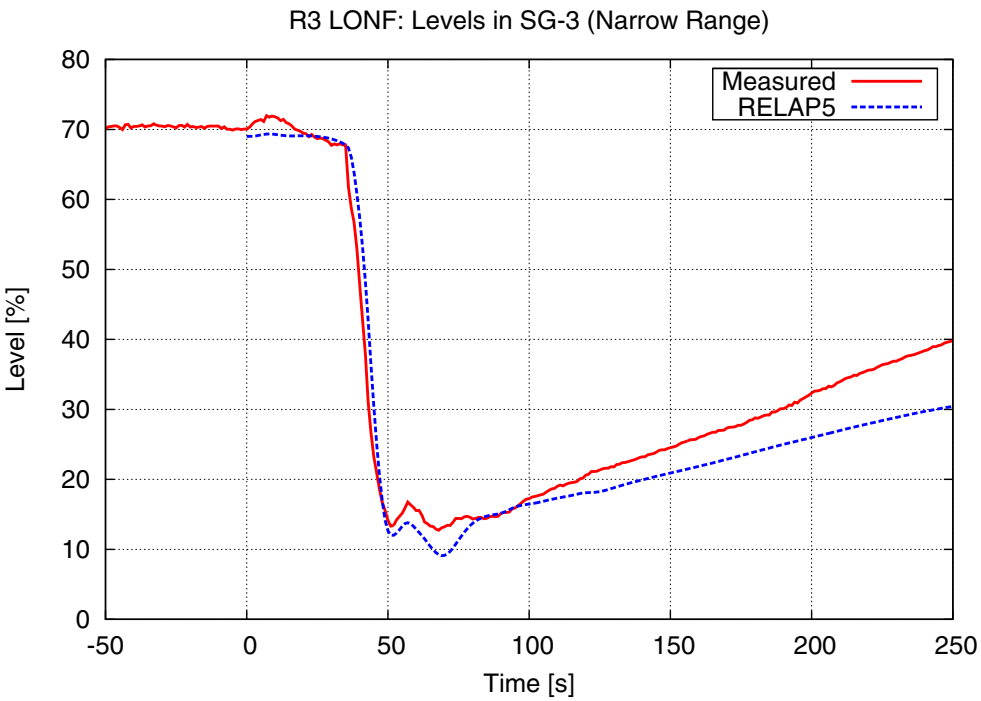

Figure 27 Narrow range level in the intact SG-3

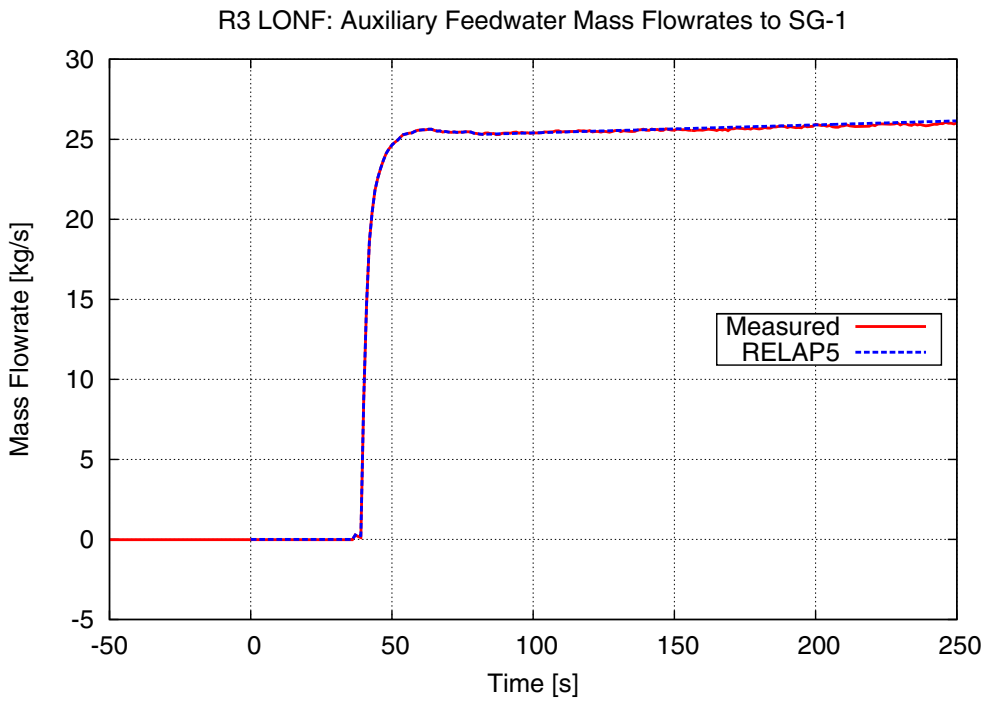

Figure 28 Auxiliary feedwater flow to the intact SG-1 (given as BC)

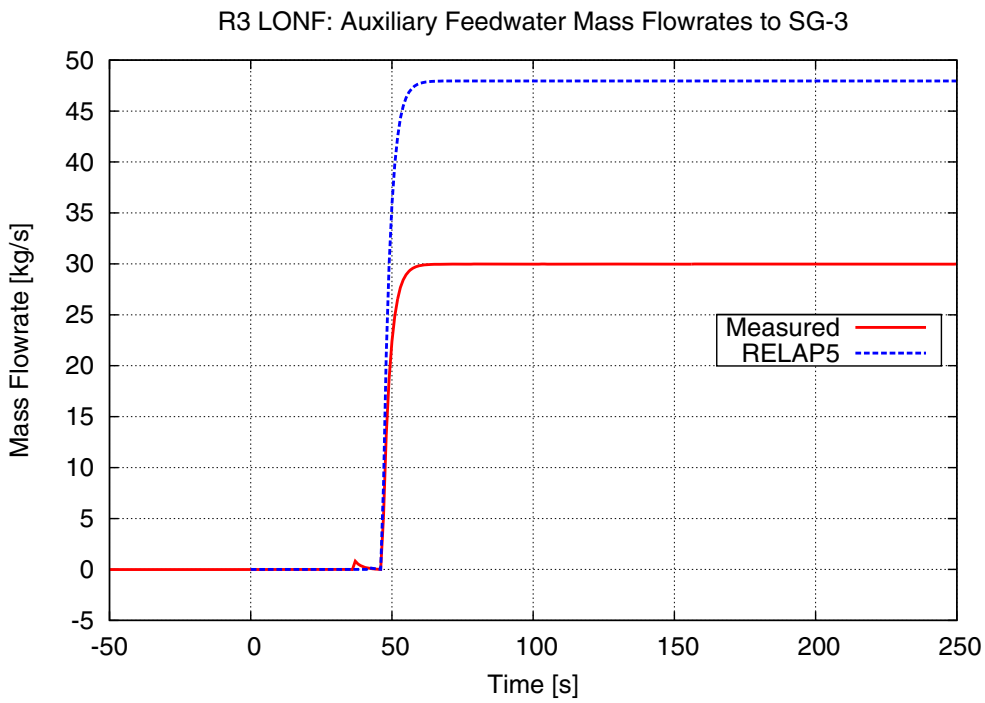

Figure 29 Auxiliary feedwater flow to the intact SG-3 (nominal value is given as BC)

Regarding some primary loop parameters, such as temperatures of the coldlegs (Figure 30 and Figure 31), the shapes of the curves are rather similar to those of the secondary side pressures shown in Figure 22 and Figure 23. This strong correlation is quite obvious because the temperature of the fluid in the returning part of the primary loop is determined by the corresponding saturation pressure in the SG.

From temperature point of view, behavior of the model is excellent. As Figure 30 and Figure 31 show, temperatures have been very well matched in the hotlegs, at both the initial and final phases of the transient. Minor discrepancies exist during the previously mentioned turbine throttling. Sudden increase of the temperature, as well as timing of the peak, has been captured properly.

In the case of the malfunctioning loop 2, the calculated initial coldleg temperature is identical with that of the intact loop 1. The real initial temperature was somewhat lower (approx. 0.6 K) due to the precursory event clarified before. After 50 s, RELAP5 slightly overestimated the temperatures in both cases but the magnitude of the discrepancy was less than 0.4 K, which was well within the measurement accuracy.

Concerning the hotleg temperatures (Figure 32 and Figure 33), the transient can be characterized by essentially 3 intervals: a nearly stationary period until the SCRAM, a large temperature drop, and a slow decrease of the temperature at the final phase. Basically, the code was capable of predicting the values very well during these stages.

Only a short delay of a few seconds duration can be observed in the timing of the sudden temperature drop. Two factors have influenced this phenomenon. The temperature measurement sensors are installed in metal pockets. Most likely, thermal inertia of the metallic structure played a role in the delay of the measured signal. In particular, magnitude of the instant cooling should be considered, which exceeded 30 K within a few seconds. On the other hand, the exact locations of the temperature measurements are just approximately known, which may result in some transition time, as well.

The 3 characteristic stages of the transient can be well distinguished in the parameters related to the pressurizer. The PRZ level (Figure 34) and pressure (Figure 35) were increasing after the transient initiation until the SCRAM signal was triggered. At this point both of the parameters decreased due to the significantly reduced heating power. With evolution of the events, lower primary system temperature resulted in a decreased volume, and this phenomenon is reflected in the PRZ level. During the final phase, the PRZ pressure was basically maintained, or even very slightly re-pressurized.

RELAP5 has managed to reproduce the parameters in PRZ very well. Magnitude of the variables, as well as the timing of the main occurrences has been captured accurately.

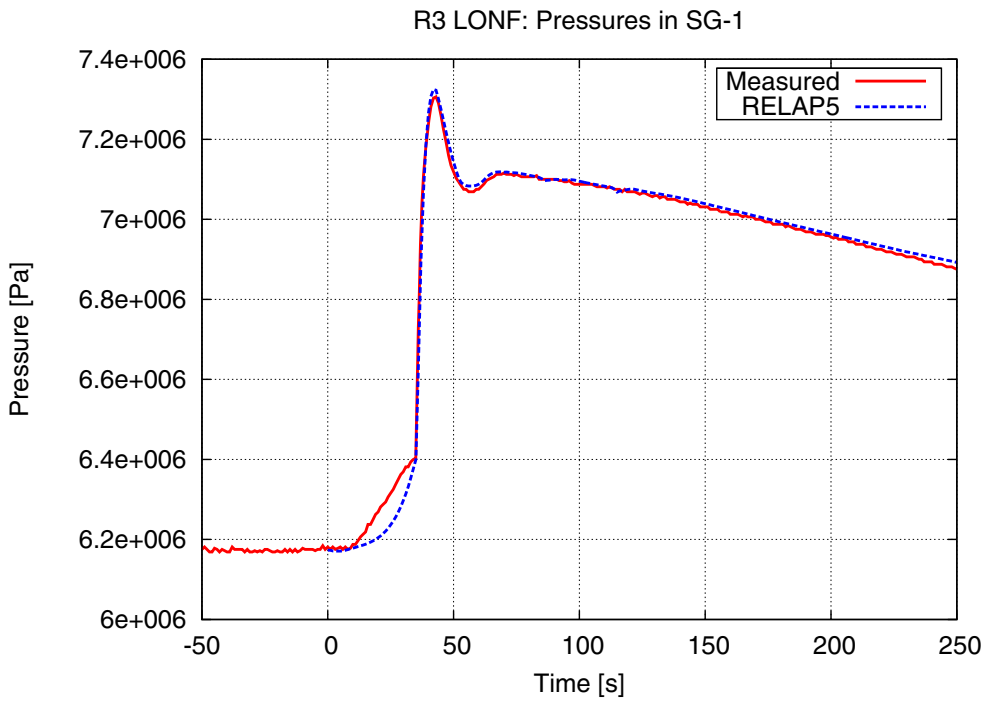

Figure 30 Coldleg temperature in the intact loop 1

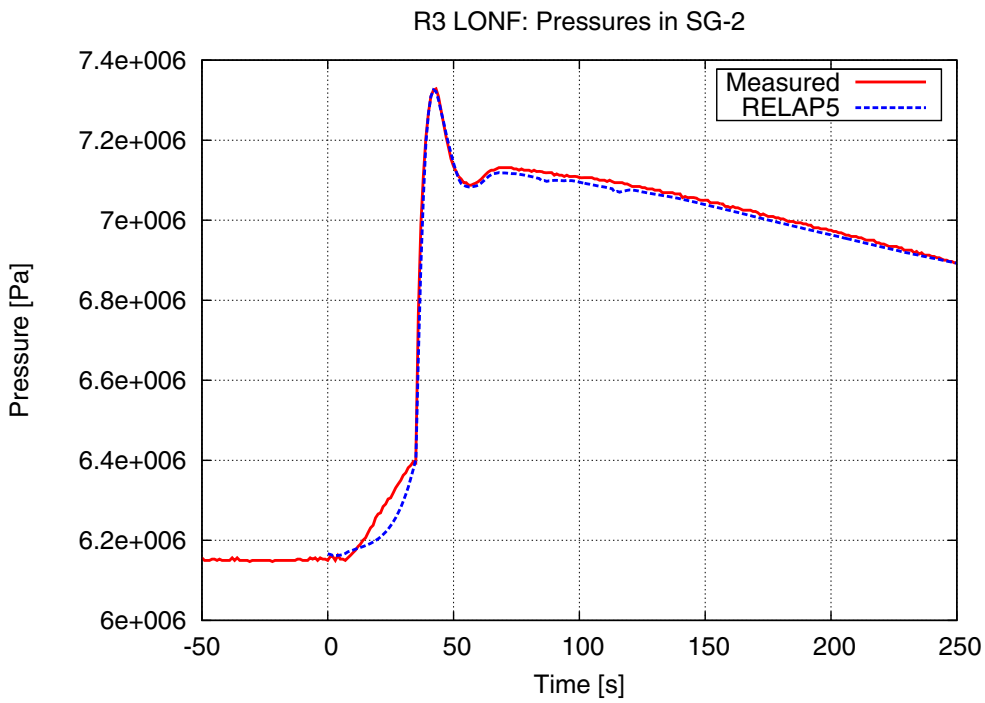

Figure 31 Coldleg temperature in the malfunctioning loop 2

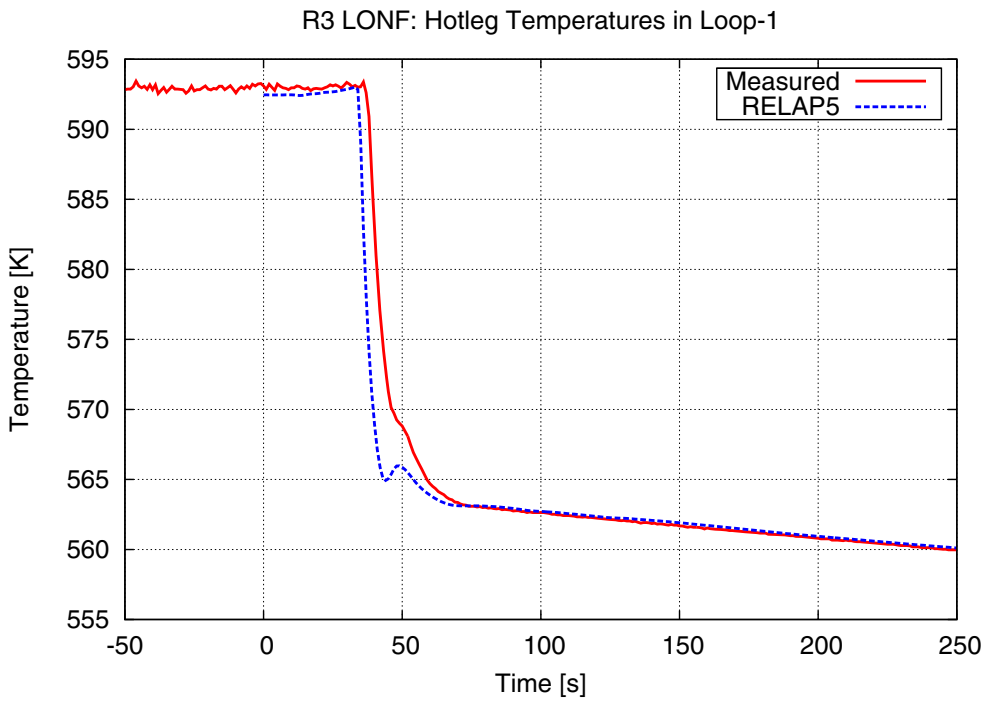

Figure 32 Hotleg temperature in the intact loop 1

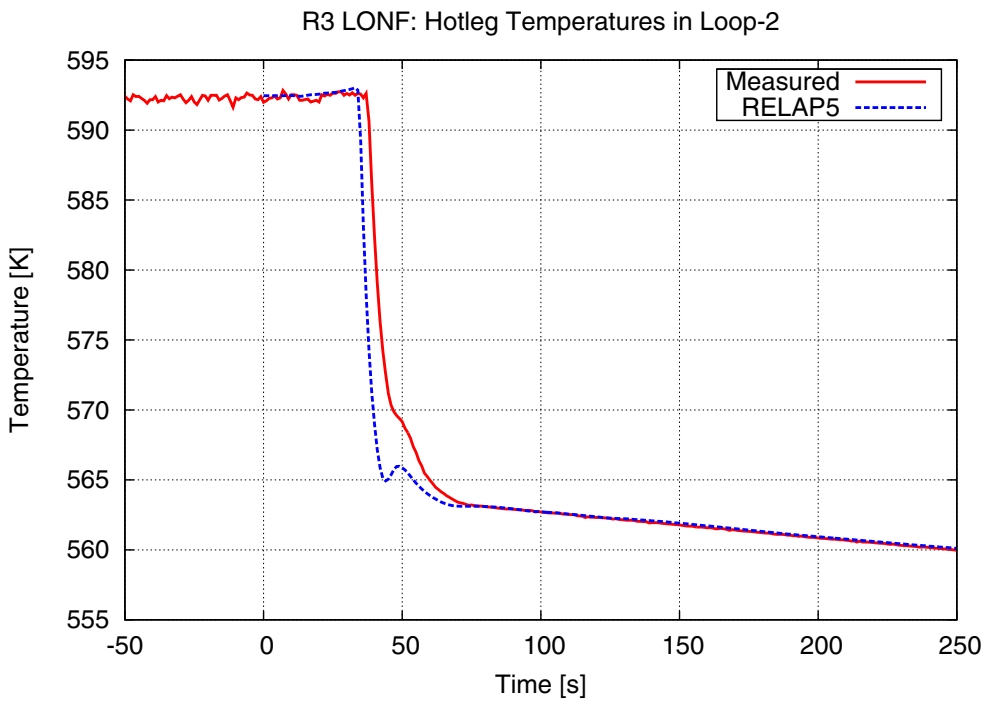

Figure 33 Hotleg temperature in the malfunctioning loop 2

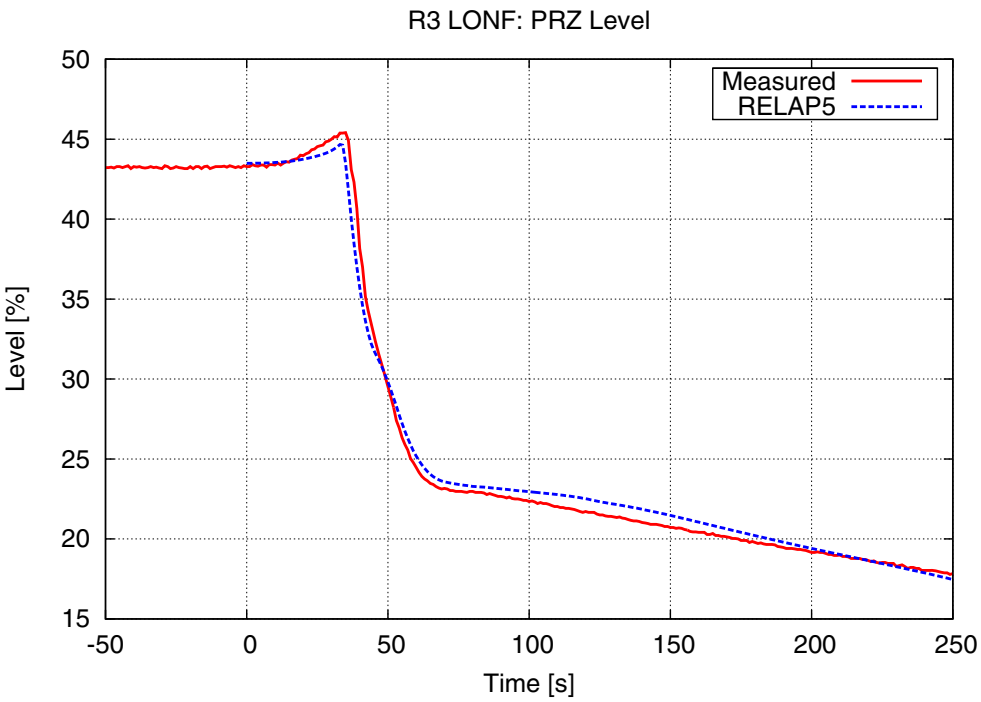

Figure 34 Level in the pressurizer

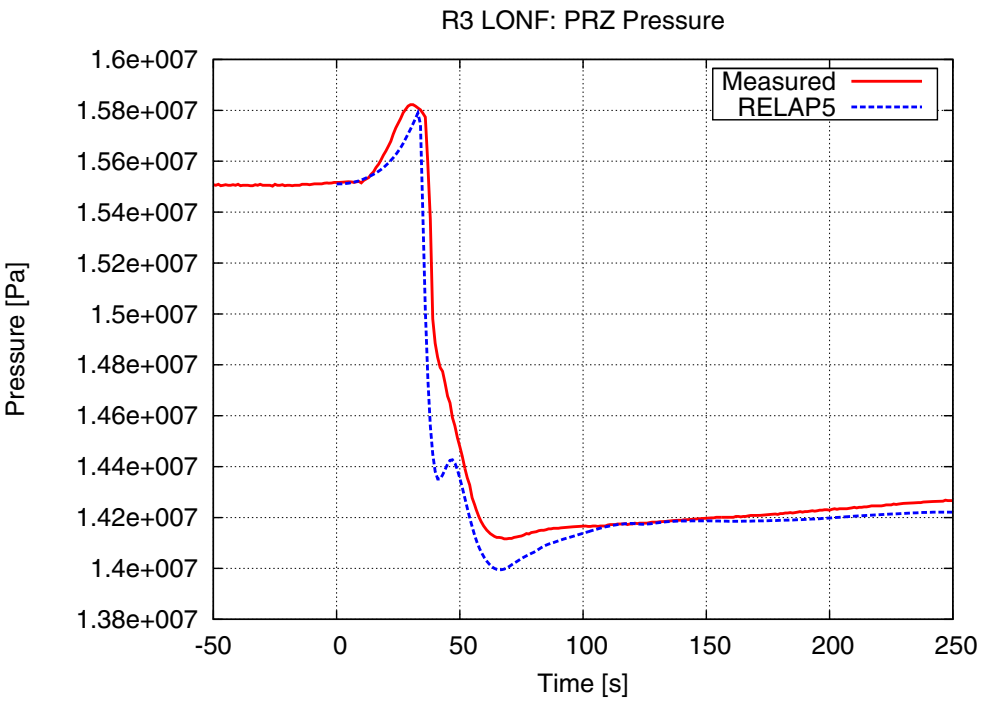

Figure 35 Pressure in the pressurizer

5. PARAMETRIC STUDY ON THE AUXILIARY FEEDWATER FLOW

Figure 36 shows the schematics of the feedwater injections to the steam generators. Normal FW became unavailable for SG-2 at the transient initiation. Soon after that, the normal FW was isolated from the other two intact SGs as well. The motor driven auxiliary feedwater system is connected to SG-1 and SG-2.

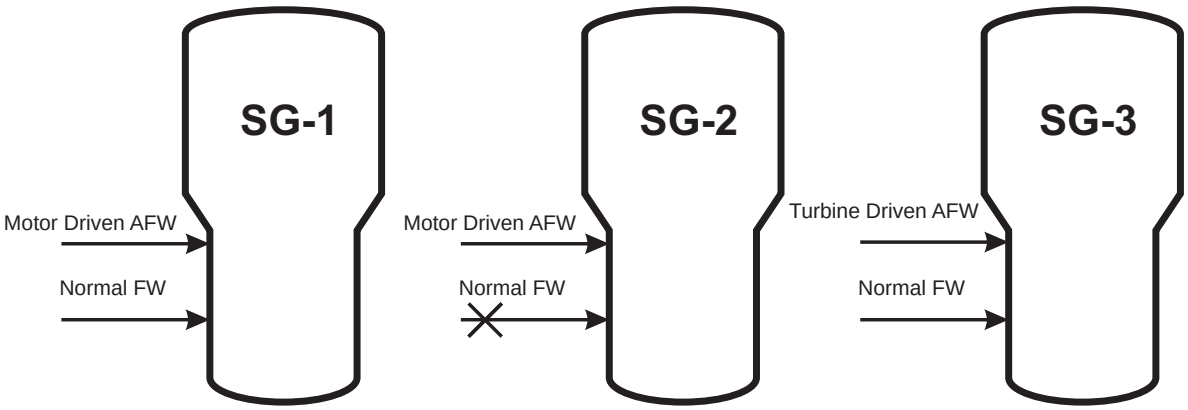

Figure 36 Arrangement of the normal and auxiliary feedwater system

The mass flowrate signals from these AFWs remained within their respective limits and provided reliable values. However, the turbine driven AFW signal became unreliable, falsely indicating that the maximal injection flowrate never exceeded approx. 30 kg/s.

During the calculations, the largest discrepancy was found between the measured and calculated values of the collapsed levels in the SG-3. Since the injected AFW flow and the corresponding SG level are strongly interrelated, it become necessary to investigate the effects of various AFW flowrates by a parametric study.

With this objective in mind, a series of calculations was accomplished over a range of different injection mass flowrates prescribed as boundary conditions. The most suitable component for this purpose was the time dependent junction no. 896 connected to SG-3. The applied user given values (Figure 37) were as follows:

1)	30 kg/s	Failed (“saturated”) measured signal
2)	48 kg/s	100 % of the nominal value (base case)
3)	60 kg/s	125 % of the nominal value
4)	72 kg/s	150 % of the nominal value

It can be seen in Figure 38 that the nominal value of the AFW resulted in an underestimation of the level. The measured quantity was well bounded by 60 kg/s and 72 kg/s, i.e. the best matching of the level is achieved with injection between 125 % and 150 % of the nominal AFW flowrate for a longer duration. However, even the constant value of 72 kg/s caused slightly slower level increase at the end of the transient.

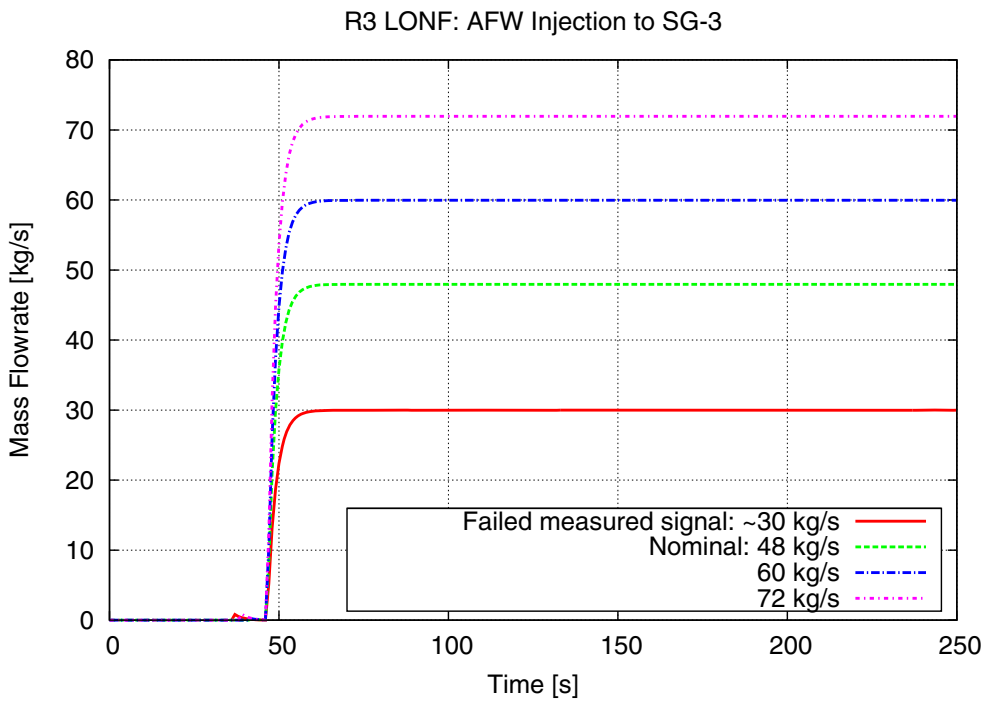

Figure 37 AFW mass flowrate as varied parameter (boundary condition)

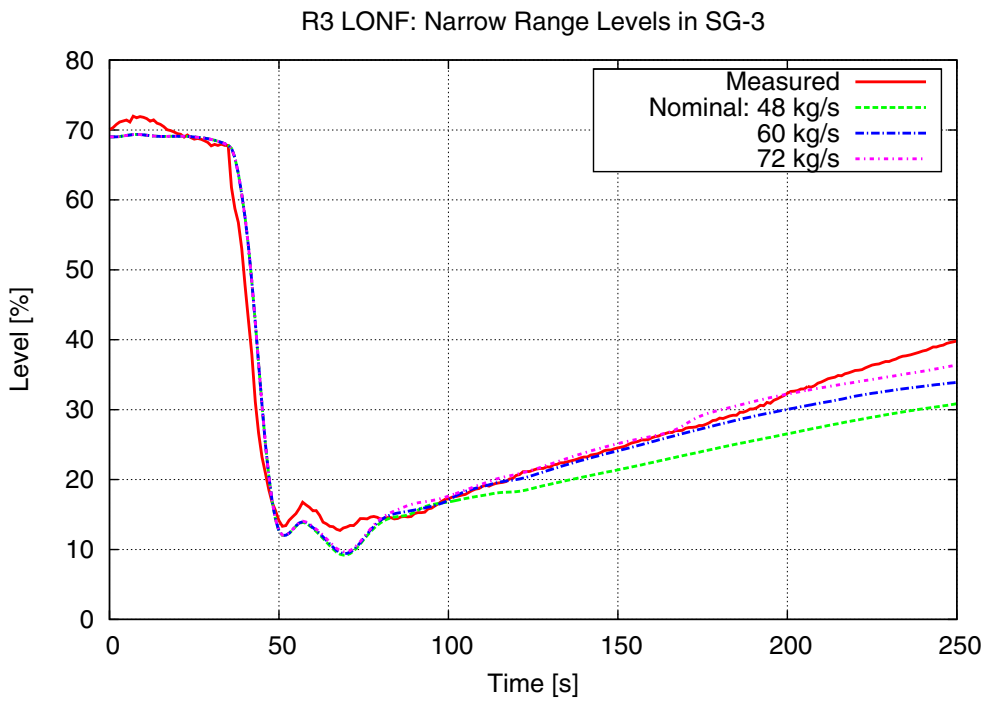

Figure 38 SG-3 level with various AFW injections

6. RUN STATISTICS

The Ringhals-3 model was imported to the SNAP graphical interface and it reported the following summary about the components in the system model (Table 3):

Table 3 Summary of the components in the model

Number of hydraulic components:	462
Accumulators	3
Annulus	7
Branches	100
ECC mixers	6
Pipes	205
Pumps	3
Single junctions	30
Single volumes	34
Separators	3
Time dependent volumes	16
Valves	45
Control systems	627
Trips	144
Control blocks	280
Signal variables	185
General tables	18
Heat Structures	200
Materials	10
Connections	1790
Control connections	751
Heat connections	365
Hydraulic connections	674

Running of the 250 s transient consumed 559.529 s of CPU time on a PC with a dual core Intel processor with 3.0 GHz speed and 3 GB RAM under a 64-bit version of MS Windows Vista.

Time-step data:

Minimum:	1.769404E-02 s
Maximum:	2.500000E-02 s
Average:	2.499750E-02 s
Requested:	2.500000E-02 s
Attempted:	22121
Successful:	22121

Mass error data:

Mass error:	3.287760 kg
Total mass:	493441.0 kg
Mass error / Total	6.662921E-06

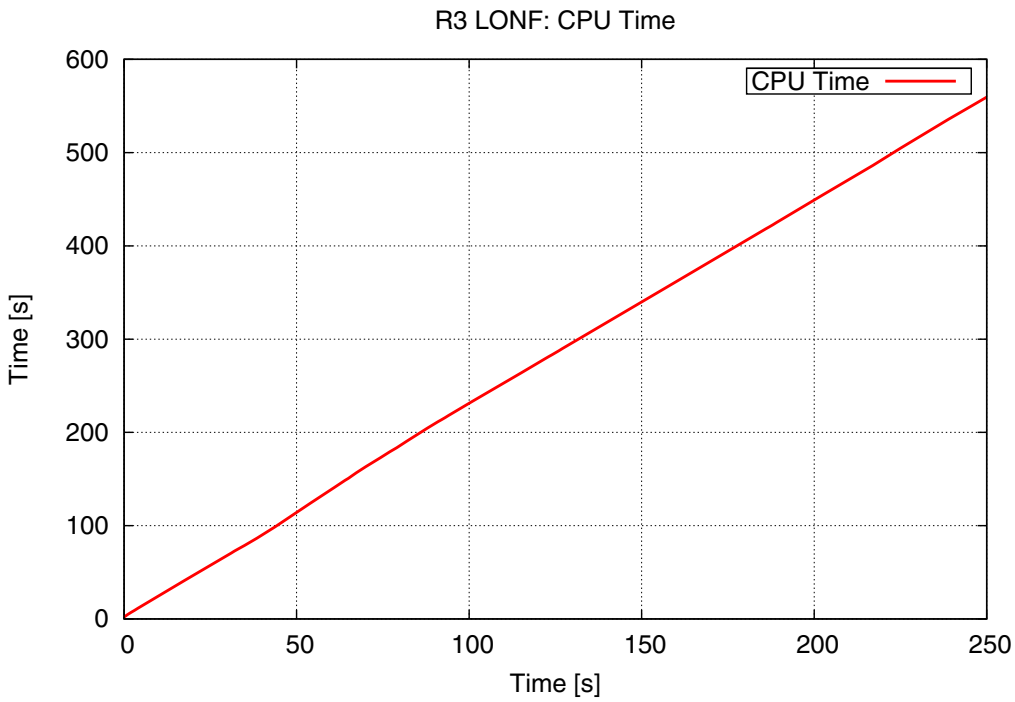

Figure 39 CPU time

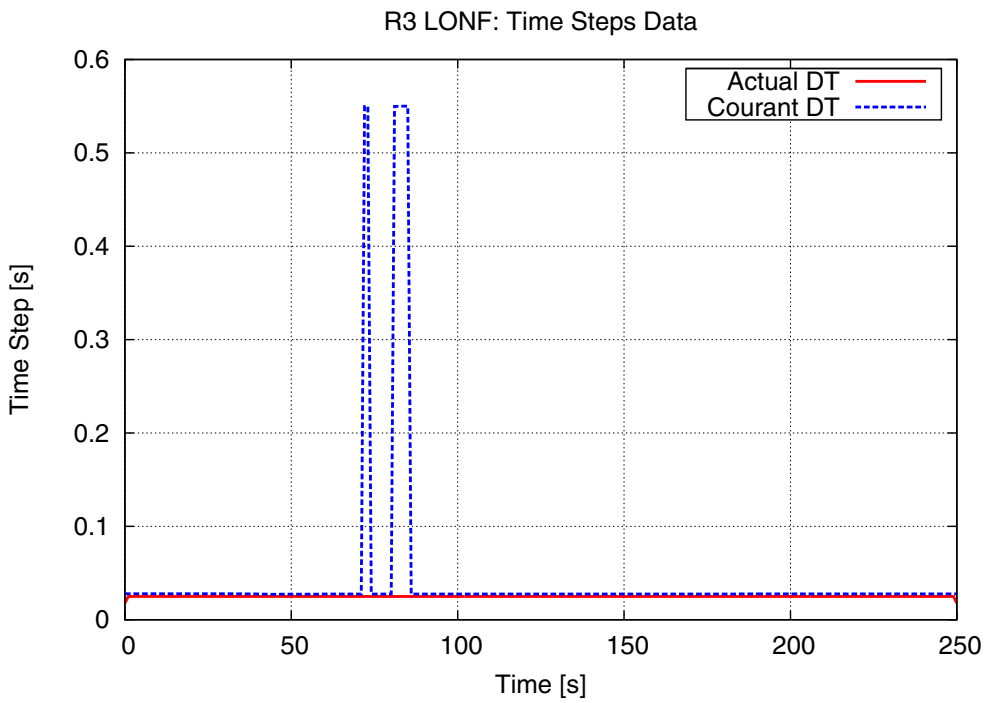

Figure 40 Actual and Courant time steps

Figure 39 indicates a smooth running transient, showing a nearly linear consumption of the CPU time. The Courant limit time-step (Figure 40) was just slightly higher than the actual time-step basically over the whole duration, except short periods between 75 – 85 s. Essentially, RELAP5 was able to run with the requested time-step, i.e. 25 ms until the end.

The calculated mass error (Figure 41) was less than 3.3 kg. This is practically negligible compared to the total system mass, because their ratio is in the order of magnitude of 10^{-6}.

There was not any sort of unphysical behavior or code failure experienced during accomplishment of the simulations. This was valid both for the command-line based execution of the code, and for using the graphical interface.

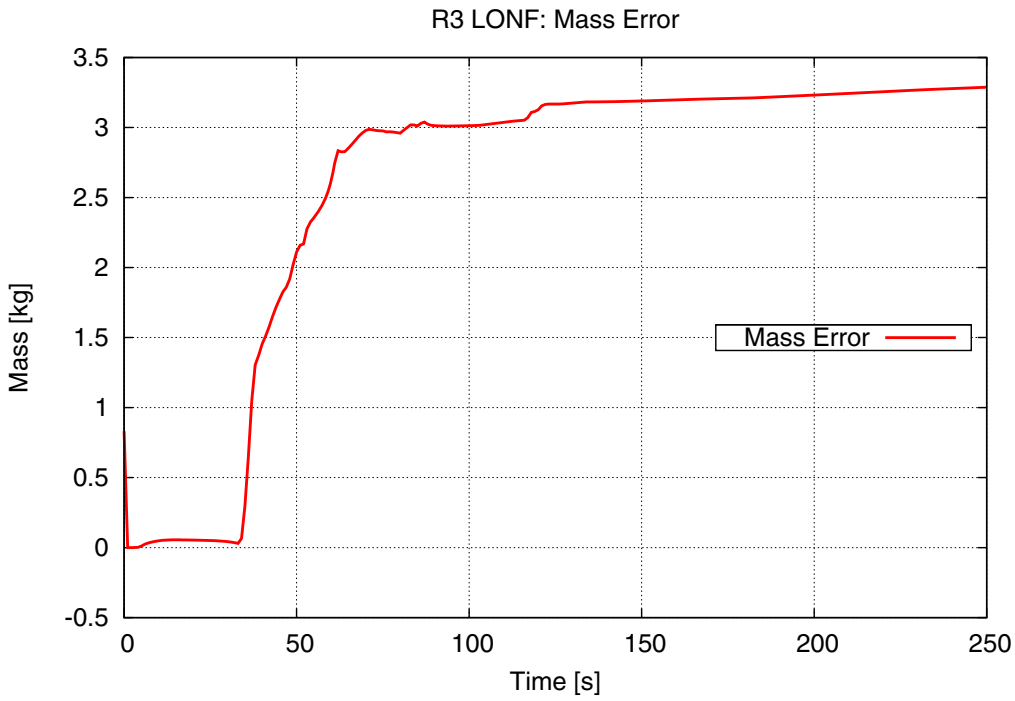

Figure 41 Mass error

6.1 Remarks on the SNAP Graphical Tool

For utilization of the Symbolic Nuclear Analysis Package, the SNAP tool, simplified animation masks were created. SNAP was found to be very useful for graphical representation of the model parameters. It helped to visualize, for instance, the fluid conditions (Figure 42), liquid temperatures, and void distribution (Figure 43). Even if the components are not proportionally scaled, a SNAP animation is extremely helpful for the analyst in better understanding of the entire process throughout a transient, such as the current Loss of Normal Feedwater scenario.

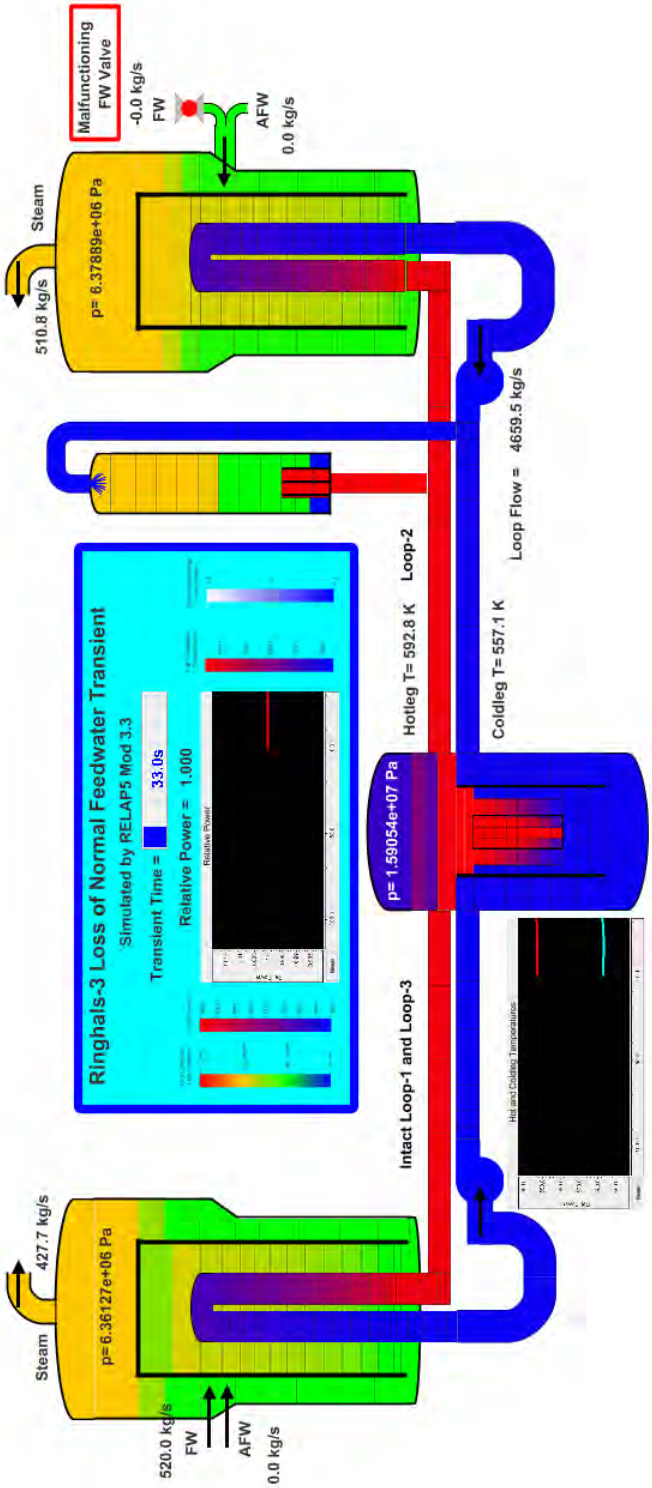

Figure 42 Animation mask with fluid conditions and temperatures

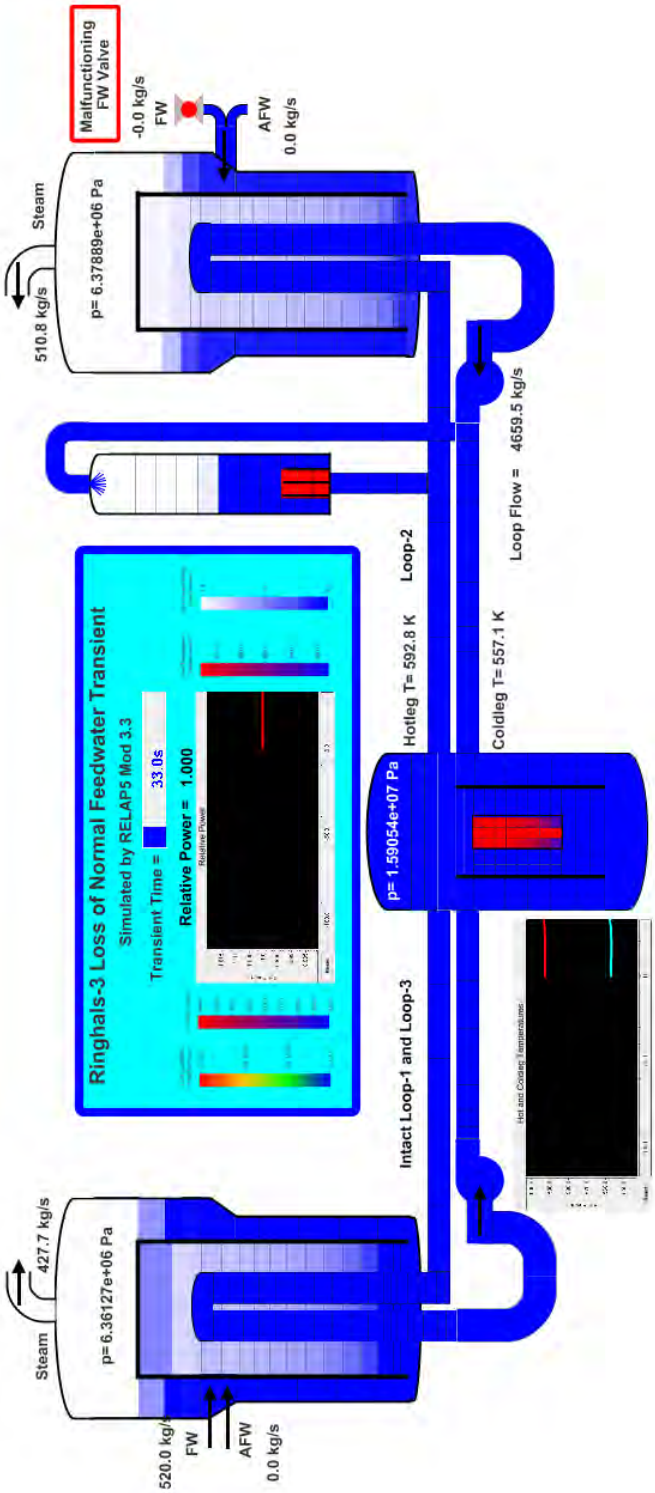

Figure 43 Animation mask with void fractions

7. CONCLUSIONS

In this report, a code validation work carried out at the Department of Nuclear Engineering, Chalmers University of Technology in the framework of the Ringhals-3 power uprate project was presented. The first phase of the project was to develop an up-to-date thermal-hydraulic model of the Ringhals-3 PWR.

With this objective in mind, a legacy RELAP5 input deck was extensively modified in order to update the input deck in accordance with the latest version of the code. One of the major improvements of the model was the complete re-nodalization of the active core. The new nodalization features a one-to-one radial mapping with the neutronic core model. Such a nodalization makes the model very versatile since all possible transients can be investigated, even in case of asymmetry between the different loops. The updated model was then successfully benchmarked against measured plant data corresponding to steady-state operation of the reactor.

The main purpose of the current validation task during transient condition was also to evaluate the capabilities of the model to reproduce the system response to a large disturbance originating from the secondary side and to test the performance of the control system and of the trip logic. Comparisons between calculations and measured data demonstrated that the RELAP5 model is able to reproduce the main plant parameters with a high level of fidelity. A few possible areas for improvement were also identified, such as improving the auxiliary feedwater injection, and better modelling the control logic of the steam dump valves.

The calculations have also revealed that the applied amount of auxiliary feedwater flow was sufficient for bringing the plant to safe shutdown conditions throughout the course of a Loss of Normal Feedwater transient. However, regaining of SG level took place at a slower pace with using the *nominal* AFW flowrate as boundary condition. Consequently, the *actual* AFW flowrate was supposedly higher than its *nominal* value specified in the plant documentation. Thus, the *nominal* AFW flowrate appears to be a conservatively underestimated quantity because, in fact, the turbine-driven AFW pump is capable of delivering more feedwater to SG-3.

8. REFERENCES

1 Image Bank of Vattenfall AB at http://www.vattenfall.com/

2 Maps at International Nuclear Safety Center: http://www.insc.anl.gov/pwrmaps/

3 Eriksson, J., "RELAP/MOD3 Base Model for the Ringhals 3/4 Plants". Technical Report, Studsvik EcoSafe, STUDSVIK/ES-94/14, 1994.

4 Stålek, M., Demazière, C., "Development and Validation of a Cross-Section Interface for PARCS", *Annals of Nuclear Energy*, 35 (2008) 2397-2409.

5 Information System Laboratories Inc., "RELAP5/MO3.3 Code Manual, Volume V: User's Guidelines", (2006), Rockville, Maryland, Idaho Falls, Idaho Falls.

6 Bánáti, J., Demazière, C., Stålek, M., 2006, "Development of a Coupled PARCS/RELAP5 Model of the Ringhals-3 PWR," Proc. of the *Int. Topical Meeting on Advances in Nuclear Analysis and Simulation* (PHYSOR2006), Vancouver, British Columbia, Canada, September 10-14, 2006.

7 Demazière, C., 2006, "Development of a Cross-Section Interface for PARCS," Proc. of the *Int. Topical Meeting on Advances in Nuclear Analysis and Simulation* (PHYSOR2006), Vancouver, British Columbia, Canada, September 10-14, 2006.

8 Demazière, C., Bánáti, J., 2006, "Application of the Coupled PARCS/RELAP5 codes for the Analysis of Transients in Connection with the Ringhals-3 Power Uprate," SKI report.

9 Bánáti, J., Demazière, C., Stålek, M., 2007, "Development and Validation of a Coupled PARCS/RELAP5 Model of the Ringhals-3 PWR," Proc. of the *15th International Conference on Nuclear Engineering* (ICONE-15), Nagoya, Japan, April 22 - 26, 2007.

10 Bánáti, J., Stålek, M., Demazière, C. and Holmgren, M.: "Analysis of a Loss of Feedwater Case at the Ringhals-3 NPP Using RELAP5/PARCS Coupled Codes", *16th International Conference on Nuclear Engineering* (ICONE-16), Orlando, FL, USA, May 11-15, 2008. Paper No.: ICONE16-48116.

11 Bánáti, J., Stålek, M., Demazière, C.: "Main Steam Line Break Calculations Using a Coupled RELAP5/PARCS Model for the Ringhals-3 Pressurized Water Reactor", *16th International Conference on Nuclear Engineering* (ICONE-16), Orlando, FL, USA, May 11-15, 2008. Paper No.: ICONE16-48702.

12 Bánáti, J., Stålek, M., Demazière, C.: "Validational Exercises with RELAP5/PARCS Coupled Codes Using Ringhals-3 Plant Data", *International Conference on Reactor Physics, Nuclear Power: A Sustainable Resource* (PHYSOR-08), Interlaken, Switzerland, Sept. 14-19, 2008.

13 Stålek, M., Bánáti, J. and Demazière, C.: "Coupled RELAP5/PARCS Main Steam Line Break Calculations Before and After a Power Uprate of a PWR", *International Conference on Reactor Physics, Nuclear Power: A Sustainable Resource* (PHYSOR-08), Interlaken, Switzerland, Sept. 14-19, 2008.

14 Ringhals AB: "Precautions, Limitations and Setpoints for Nuclear Steam Supply and Balance of Plant Systems", Document ID: 1611225, Version: 18.0, 2004.